Faraday effect and multiple scattering of light

A. S. Martinez* and R. Maynard

Laboratoire d'Expérimentation Numérique and Centre de Recherche sur les Très Basses Températures, Maison des Magistères, Centre National de la Recherche Scientifique, Boîte Postale 166, 38042 Grenoble Cedex 9, France

(Received 27 July 1993; revised manuscript received 8 March 1994)

The presence of a magnetic field in an optically active medium produces a rotation of the polarization of light: it is the well-known Faraday effect, which breaks the time-reversal symmetry. The averaged light intensity in the multiple scattering of light by disordered systems is described by the weak-localization theory based on the direct and reverse sequences of scatterings, which are founded on the time-reversal symmetry. The multiple scattering of electromagnetic (vectorial) waves by spherical particles is considered in the presence of a magnetic field. We have shown that the electric field of the reversed path can be obtained from the direct one by a simple matrix transposition. In systems of reduced dimensionality (1 and 2), we have shown that for the same polarization channel, the peak of the backscattering cone is not affected by the Faraday effect even though the time-reversal symmetry is broken. The intensity correlation function is obtained for a one-dimensional system. This simple model furnishes two results: (i) even though the wave vector is randomized, there is no decorrelation of the polarization for paths of the same length and (ii) the correlation function has an oscillatory behavior as a function of the magnetic field. In three dimensions, we have calculated analytically the attenuation of the backscattering cone as well as the decorrelation length for the multiple Rayleigh scattering. Mie scattering has been considered by Monte Carlo simulations. In the diffusion regime (thick slabs) our results are in accord with previous results and with experiments. Nevertheless, for the intermediate regime in transmission, we have found oscillations of the intensity correlation as a function of the magnetic field. For reflection and strong magnetic field, we have observed the convergence of the enhancement factor to nontrivial asymptotic values.

INTRODUCTION

The multiple scattering of waves is a phenomenon which appears in very distinct physical systems[1] such as the propagation of sound waves or light through a suspension of scattering particles, emulsions, and clouds, but it also appears in the propagation of electron wave functions in impure metals or semiconductors.[2] Several recent advances have been made in the description of the multiple scattering of waves, such as, for example, the existence of the reverse scattering sequence accompanying the direct one in reflection geometry.[3] The presence of these two sequences leads to the backscattering cone which is an enhancement of the intensity of light by a factor of 2 in the backscattering direction.

The multiple scattering of waves can be analyzed at several levels. The simplest one is to consider the approximation of scalar waves which are elastically scattered by pointlike inhomogeneities. Although these approximations can take into account the weak-localization phenomenon (the backscattering cone, for example), the assumption of scalar waves (and pointlike scatterers) is not realistic for light. Most experiments are indeed performed with polarized light (vectorial nature of the electromagnetic field) which are scattered by finite-size spheres. A deeper level of analysis is then necessary. Actually, the study of polarized light scattered by spherical particles is possible. The scattering amplitudes are rather complex mathematical functions, given by the Mie theory.[4] Nevertheless, numerical simulations (of the Monte Carlo type for instance) furnish an efficient way to tackle this difficult problem.[5]

Although the strong localization of light has not been unambiguously observed in three dimensions, in the context of weak localization, the destruction of the wave interference phenomenon by the application of a magnetic field has already been proposed and very recently measured.[6–8] The understanding of this essentially vectorial phenomenon, which breaks the time-reversal symmetry, may constitute an important step in the comprehension of the multiple scattering of light, since it is the only physical effect which affects the intensity of the backscattering peak. We notice that absorption or reduced geometry leads to a rounding of this peak rather than an attenuation.

The previous theories of the Faraday effect in multiple-scattering media assume that the helicity states of polarization are random variables, independent of the direction of the wave vector. These helicity states jump randomly from one state (say, $+1$) to the other (-1). This stochasticity is introduced on purpose to provide a global damping of correlation functions in a quite phenomenological way. Nevertheless, the polarization states are not random variables, but follow the random changes of the wave vector through the scattering amplitude matrix. Here, we have considered a model with better physical foundation.

This paper is organized in the following way. In Sec. I, general results of the Faraday effect in multiple scattering are discussed. The purpose of this discussion is to define carefully the nature of the symmetry breaking between the direct and the reverse multiple-scattering sequences under a magnetic field. In Sec. II, the problem of one-dimensional anisotropic multiple scattering is treated. Due to the simplicity of the model, an exact solution can be obtained, which shows that, despite the random-walk nature of the multiple-scattering paths, a strong correlation subsists on the length of these paths. In Sec. III, we consider the Faraday effect in three-dimensional multiple Rayleigh scattering. By using recursive relations, it is possible to obtain the solutions for the Stokes intensities as well as the different correlation functions in transmission and reflection as a function of the magnetic field B. For reflection, we find an exponential damping [varying as $n(B\ell)^2$, where n is the number of scatterings and ℓ the mean free path] and asymptotic nontrivial values for large values of B. For transmission, we find that the correlation function decays exponentially as $n(B\ell)^2$ which is an envelope for the oscillations. In Sec. IV, we consider multiple Mie scattering using a Monte Carlo algorithm. Comparison with experiments is made. For transmission, we discuss the origin of the oscillations of the correlation function reported in Ref. 9.

I. GENERAL RESULTS ON THE FARADAY EFFECT IN MULTIPLE SCATTERING

We consider a slab of thickness L with infinite planes parallel to the $(x\text{-}y)$ plane. This slab contains randomly distributed spheres and a magnetic field B is applied along the z direction. A photon is injected along the z axis and it is multiply scattered by the spheres. The mean free path is $\ell=1/\rho\sigma$, where ρ is the density of spheres in the slab and σ the total scattering cross section. The detection of the emergent beam is also along the z axis, either in transmission or in reflection.

The magnetic field in an optically active material produces different refractive indexes for right- and left-handed circular polarization, producing different velocities of propagation. Since any polarization state is the combination of these two circular states, the effect of a magnetic field can be described alternatively in a rectangular basis by a rotation of the polarization state (Faraday rotation) by an angle $\alpha=V\mathbf{B}\cdot\hat{k}r$ where V is the Verdet constant, $\mathbf{B}$ the magnetic field, $\hat{k}$ the unitary wave vector, and r the distance between two scatterings.[10] The helicity states are conjugated by the time-reversal symmetry and their different behavior under a magnetic field corresponds to a time-reversal symmetry breaking. Moreover, an important feature of the Faraday effect is the failure of the reciprocity theorem due to the nonsymmetric permeability tensor of a gyromagnetic medium.

In the limit of weak disorder, we can assume independent multiple-scattering sequences, and for each sequence we can assume that the scatterings happen in the far-field limit, so that the longitudinal component of the electric field can always be ignored (Fig. 1). In this case, the electric field after $n-1$ scatterings is given in the "scattering plane" representation by

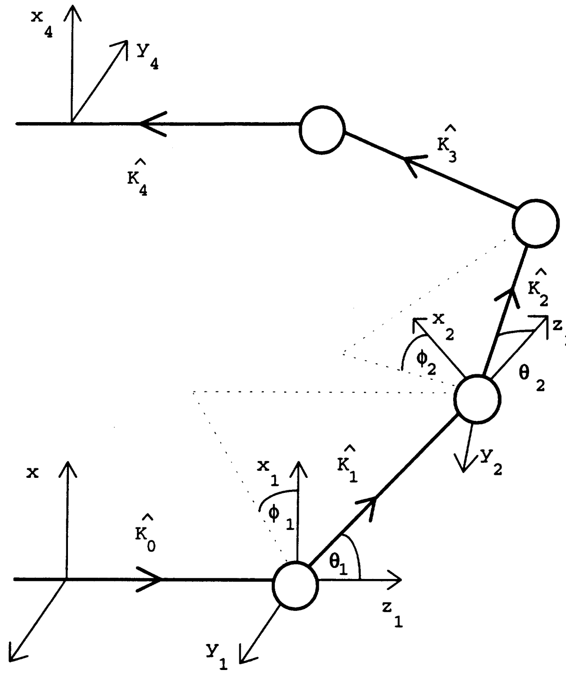

FIG. 1. Representation of a sequence of four scatterings in reflection. The laboratory frame (x,y,z) is represented in the beginning of the sequence. The first two local frames (x_1,y_1,z_1) and (x_2,y_2,z_2) are also represented. The exit intensity is measured in the frame (x_4,y_4,z_4) which is an improper rotation of the laboratory frame. The scattering planes are represented for the first and second scatterings.

$$\begin{bmatrix} E_{nx} \\ E_{ny} \end{bmatrix} = R(\alpha_n)\prod_{\kappa=1}^{n} -j\frac{\exp(-jkr_\kappa)}{kr_\kappa}J(\cos\theta_\kappa) \times R(\alpha_{\kappa-1}-\phi_\kappa)\begin{bmatrix} E_{ox} \\ E_{oy} \end{bmatrix}, \tag{1.1a}$$

where the order of the product is important. It starts with the first term $(\kappa-1)$ in the right-hand side. Here $j=\sqrt{-1}$,

$$R(\alpha)=\begin{bmatrix} \cos\alpha & -\sin\alpha \\ \sin\alpha & \cos\alpha \end{bmatrix} \tag{1.1b}$$

and

$$J(\cos\theta)=\begin{bmatrix} S_\parallel(\cos\theta) & 0 \\ 0 & S_\perp(\cos\theta) \end{bmatrix}, \tag{1.1c}$$

where two consecutive wave vectors $\hat{k}_{\kappa-1}$ and $\hat{k}_\kappa$ define the κth scattering plane. The scattering angles $\theta_\kappa=\arccos(\hat{k}_{\kappa-1}\cdot\hat{k}_\kappa)$ can take continuous values in the interval $[0,\pi]$. The azimuthal angles ϕ_κ take continuous values in the interval $[0,2\pi]$ and project the electric field along the parallel and perpendicular directions of the κth scattering plane. These components are then scattered with amplitudes $S_\parallel(\cos\theta)$ and $S_\perp(\cos\theta)$, respectively, given by the Mie theory of scattering.[4] Notice that the last scattering angles θ_n and ϕ_n are not random since the detection is fixed to be perpendicular to the slab. The matrix J is diagonal because of the spherical symmetry of the scatterers but it does not commute with the rotation matrix, so that we cannot simply compose the rotations. Furthermore, the intermediate electric fields are given in their local basis, the basis $(\hat{\theta}_\kappa,\hat{\phi}_\kappa,\hat{k}_\kappa)$.

The "scattering plane" frame representation of the multiple scattering is the simplest basis to write the Jones matrix. But in the multiple-scattering regime, this simplification is only apparent since after each scattering we must keep track of the transformation of the local frame to the laboratory one (x,y,z) in order to impose the condition that the photon quits the slab with a wave vector normal to the slab plane. It is better suited for the present problem to use the Chandrasekhar-Sekera representation.[11] Although algebraically more complicated, in this representation the wave vectors $\hat{k}_\kappa$ are always given in the laboratory basis by the spherical angles Θ_κ and Φ_κ and the fields are given along the direction $(\hat{\Theta}_\kappa,\hat{\Phi}_\kappa)$.

A. Single scattering

Let us first consider $B=0$ and a single scattering from the incident wave vector $\hat{k}_0$ to $\hat{k}_1$. The scattered field E_1 is obtained from the incident one E_0 through the Jones matrix

$$J(\hat{k}_1,\hat{k}_0)=\begin{bmatrix} j_{11} & j_{12} \\ j_{21} & j_{22}\end{bmatrix} . \tag{1.2a}$$

Its elements can be obtained from Eqs. (1.1) in the Chandrasekhar-Sekera representation. Following the notation used by Cheung and Ishimaru,[12]

$$\begin{aligned} j_{11}&=(l,l)X_1+(r,r)X_2, \quad j_{12}=-(r,l)X_1+(l,r)X_2 , \\ j_{21}&=-(l,r)X_1+(r,l)X_2, \quad j_{22}=(r,r)X_1+(l,l)X_2 , \end{aligned} \tag{1.2b}$$

with

$$\begin{aligned} (l,l)&=\sqrt{(1-\mu_0^2)(1-\mu_1^2)}+\mu_0\mu_1\cos(\Delta\Phi) , \\ (l,r)&=-\mu_0\sin(\Delta\Phi) , \\ (r,l)&=\mu_1\sin(\Delta\Phi), \quad (r,r)=\cos(\Delta\Phi) , \end{aligned} \tag{1.2c}$$

$$\begin{aligned} X_1&=\frac{S_\perp(\cos\theta)-\cos\theta\, S_\parallel(\cos\theta)}{\sin^2\theta} , \\ X_2&=\frac{S_\parallel(\cos\theta)-\cos\theta\, S_\perp(\cos\theta)}{\sin^2\theta} , \end{aligned} \tag{1.2d}$$

and

$$\cos\theta=\sqrt{(1-\mu_0^2)(1-\mu_1^2)}\cos(\Delta\Phi)+\mu_0\mu_1 , \tag{1.2e}$$

with $\mu_1=\cos\Theta_1$, $\mu_0=\cos\Theta_0$, and $\Delta\Phi=\Phi_0-\Phi_1$, where Θ_0,Φ_0 and Θ_1,Φ_1 are the polar angles of the incident wave vector $\hat{k}_0$ and the scattered wave vector $\hat{k}_1$ in the laboratory frame, respectively. The electric field is now given in the basis of the wave vectors, i.e., along the directions $\hat{\Theta}_1$ and $\hat{\Phi}_1$. The reverse scattering is obtained by changing $\hat{k}_1'=-\hat{k}_0$ and $\hat{k}_0'=-\hat{k}_1$, implying that $\Theta_1'=\pi-\Theta_0$, $\Theta_0'=\pi-\Theta_1$, $\Phi_0'=\pi+\Phi_1$, and $\Phi_1'=\pi+\Phi_0$; consequently, $\mu_1'=-\mu_0$, $\mu_0'=-\mu_1$, and $\Delta\Phi'=-\Delta\Phi$, leading to $(l,l)'=(l,l)$, $(r,r)'=(r,r)$, $(l,r)'=-(r,l)$, and $(r,l)'=-(l,r)$, and finally $j_{11}'=-j_{11}$, $j_{22}'=-j_{22}$, $j_{12}'=-j_{21}$, and $j_{21}'=-j_{12}$.

Now let us define the "antitransposition" of a matrix A by the relation

$$A^{(\mathrm{at})}=\text{Antitransposition}\left[\begin{bmatrix} a_{11} & a_{12} \\ a_{21} & a_{22}\end{bmatrix}\right] \equiv \begin{bmatrix} a_{11} & -a_{21} \\ -a_{12} & a_{22}\end{bmatrix} . \tag{1.3a}$$

This operation has the property

$$(AB)^{(\mathrm{at})}=B^{(\mathrm{at})}A^{(\mathrm{at})} . \tag{1.3b}$$

The Jones matrix of the reverse scattering is nothing else than the *antitransposition* of the Jones matrix of the direct scattering:

$$J(-\hat{k}_0,-\hat{k}_1)=J^{(\mathrm{at})}(\hat{k}_1,\hat{k}_0)=\begin{bmatrix} j_{11} & -j_{21} \\ -j_{12} & j_{22}\end{bmatrix} . \tag{1.4}$$

Let us now consider the situation where the medium is magneto-optically active while the scatterers are insensitive to the magnetic field. The magnetic field is applied along the incident direction $(\hat{k}_0)$. The Faraday effect rotates the polarization in the plane perpendicular to the wave vector. For the direct scattering we have $R(\alpha_1)J(\hat{k}_1,\hat{k}_0)R(\alpha_0)$. Let us consider two particular situations: the forward and the backward scattering. The Mie theory for the forward scattering $(\hat{k}_1=\hat{k}_0)$ states that $S(1)=S_\parallel(1)=S_\perp(1)$ so that $J(\hat{k}_0,\hat{k}_0)=S(1)I$ with

$$I=\begin{bmatrix} 1 & 0 \\ 0 & 1\end{bmatrix} .$$

For this situation, $R(\alpha_0)$ commutes with J which leads to an effective Jones matrix proportional to $R(\alpha_0+\alpha_1)$. For the backward scattering $(\hat{k}_1=-\hat{k}_0)$, the Mie theory states that $S(-1)=S_\parallel(-1)=-S_\perp(-1)$ so that $J(-\hat{k}_0,\hat{k}_0)=S(-1)\sigma_z$, where

$$\sigma_z=\begin{bmatrix} 1 & 0 \\ 0 & -1\end{bmatrix}$$

is the Pauli matrix. The effective Jones matrix is then proportional to

$$R(-\alpha_1)\sigma_z R(\alpha_0)=\sigma_z R(\alpha_0+\alpha_1) .$$

We stress that (i) we have written $-\alpha_1$ because $\hat{k}_1$ is antiparallel to the magnetic field and (ii) in this case, the detection is in a frame obtained by an improper rotation of the laboratory frame (x,y,z). The presence of σ_z is a signature of this improper rotation. Hence the Faraday rotation is always of $\alpha_0+\alpha_1$ in the forward and backward scattering cases.

For a more general case, where $\hat{k}_0$ and $\hat{k}_1$ are not aligned, the reverse scattering is described by an effective Jones matrix,

$$R(-\alpha_0)J(-\hat{k}_0,-\hat{k}_1)R(-\alpha_1) = [R(-\alpha_1)J(\hat{k}_1,\hat{k}_0)R(-\alpha_0)]^{(\mathrm{at})} .$$

In the presence of a magnetic field there is a simple relation between the scattered field of the direct and reverse scatterings. The effective Jones matrix of the reverse scattering is obtained by antitransposing the effective Jones matrix of the direct scattering but changing $\mathbf{B}$ into $-\mathbf{B}$.

B. Multiple scattering

Consider now a scattering sequence characterized by the wave vectors

$$\{\hat{k}_0 \to \hat{k}_1 \to \hat{k}_2 \to \cdots \to \hat{k}_n = \pm\hat{k}_0\} ,$$

where the sign $\pm$ corresponds respectively to the transmission or reflection through a slab of length L where the magnetic field is aligned along the z axis ($\hat{k}_0$). The emerging electric field in *transmission* is obtained by the application of the effective Jones matrix,

$$J_{\mathrm{trans}} = R(\alpha_n)J(\hat{k}_0,\hat{k}_{n-1}) \cdots R(\alpha_2) \times J(\hat{k}_2,\hat{k}_1)R(\alpha_1)J(\hat{k}_1,\hat{k}_0)R(\alpha_0) , \tag{1.5}$$

to the incident field.

In reflection, the detection is not performed in the laboratory frame but in the frame obtained by an improper rotation of it (Fig. 1). The emerging electric field is obtained by the effective Jones matrix $J_{\mathrm{ref}} = J_{\mathrm{dir}} + J_{\mathrm{rev}}$, where J_{dir} and J_{rev} are the contributions of the direct and reverse sequences, respectively. The contribution of the *direct* sequence to the effective Jones matrix is

$$J_{\mathrm{dir}} = R(\alpha_n)J(-\hat{k}_0,\hat{k}_{n-1}) \cdots R(\alpha_2) \times J(\hat{k}_2,\hat{k}_1)R(\alpha_1)J(\hat{k}_1,\hat{k}_0)R(\alpha_0) . \tag{1.6a}$$

The reverse sequence

$$\{\hat{k}_0 \to -\hat{k}_{n-1} \to -\hat{k}_{n-2} \to \cdots \to -\hat{k}_1 \to -\hat{k}_0\}$$

subsists with the same weight as the direct one even when the ensemble average is performed. Notice that for the intensities, it is well known from the Bethe-Salpeter equation that the intensity of the direct sequence plus the intensity of the reverse sequence equals the ladder diagrams; the crossed diagrams equal the intensity of the interference between the amplitudes of the direct and reverse paths. The contribution of the *reverse* sequence is

$$J_{\mathrm{rev}} = R(-\alpha_0)J(-\hat{k}_0,-\hat{k}_1) \cdots R(-\alpha_{n-2}) \times J(-\hat{k}_{n-2},-\hat{k}_{n-1})R(-\alpha_{n-1}) \times J(-\hat{k}_{n-1},\hat{k}_0)R(-\alpha_n) . \tag{1.6b}$$

Using the property Eq. (1.3b) one can write

$$J_{\mathrm{rev}} = [R(-\alpha_n)J(-\hat{k}_0,\hat{k}_{n-1}) \cdots R(-\alpha_2)J(\hat{k}_2,\hat{k}_1) \times R(-\alpha_1)J(\hat{k}_1,\hat{k}_0)R(-\alpha_0)]^{(\mathrm{at})} , \tag{1.6c}$$

since $R(\alpha) = R^{(\mathrm{at})}(\alpha)$. This expression can be written as

$$J_{\mathrm{rev}}(B) = J_{\mathrm{dir}}^{(\mathrm{at})}(-B) . \tag{1.6d}$$

The previous expression shows clearly the effect of the magnetic field when compared to the direct sequence: the rotation angles are the opposite while the matrix product has to be antitransposed. This leads to $J_{\mathrm{rev}} \neq J_{\mathrm{dir}}$, the effect of the time-reversal symmetry breaking. Indeed, in the absence of a magnetic field ($\alpha_\kappa = 0$), we have obtained a very general result, which is independent of the dimensionality of the system. The effective Jones matrix of the reverse sequence is simply given by the antitransposition of the effective Jones matrix of the direct sequence.

Consider now the situation where the electric field is propagating in three dimensions but the scatterers are located in a lower-dimensional space [along the z axis in one dimension or on the (x-z) plane in two dimensions]. In one dimension, only forward and backward scatterings may occur so that the Jones matrices are diagonal. In two dimensions, the angles ϕ_κ can take only two values, either 0 or π, implying that $\Delta\Phi = 0$ or π; consequently the off-diagonal terms (r,l) and (l,r) vanish in Eq. (1.2b). In one and two dimensions, because the Jones matrices are diagonal, one can write $J(-\hat{k}_{\kappa-1},-\hat{k}_\kappa) = J(\hat{k}_\kappa,\hat{k}_{\kappa-1})$ and using that $R^{(t)}(-\alpha) = R(\alpha)$, where (t) stands for the transposition operation, one obtains

$$J_{\mathrm{rev}}(\mathbf{B}) = J_{\mathrm{dir}}(\mathbf{B}), \quad \text{one dimension} , \tag{1.7a}$$

and

$$J_{\mathrm{rev}}(\mathbf{B}) = J_{\mathrm{dir}}^{(t)}(\mathbf{B}), \quad \text{two dimensions} . \tag{1.7b}$$

We point out that in the scalar approximation only the phases are important, and the reverse sequence is obtained by changing both the order of the matrix product and $\hat{k}_\kappa \to -\hat{k}_\kappa$. In this case, the reverse sequence is equivalent to the time-reversed one. For vectorial waves the time-reversed sequence is different from the reverse sequence. The breaking of the time-reversal symmetry calls for some comments. Two experimental situations must be distinguished: (i) *the backscattering configuration,* where the initial polarization state of the direct and reverse sequences is the same, and (ii) *the reciprocal configuration,* where the initial polarization state of the reverse sequence is the outcoming polarization of the direct sequence (this can be achieved by mirroring the end of the direct sequence, as in the ultrasound experiment of the time-reversal mirror[13]). The Faraday effect does break the time-reversal symmetry but it does not necessarily affect the coherent backscattering cone for one and two dimensions as we will show. This is a consequence of the unexpected relations (1.7a) and (1.7b).

We stress that the above results are not dependent on the size of the spheres. Motivated by the recent experiments of Erbacher, Lenke, and Maret,[8,14] we are interested in the enhancement factor of the backscattering cone for the reflection experiment and in the intensity correlation function for the transmission one.

C. Enhancement factor

The enhancement factor is defined as

$$\Xi_{\text{out,in}}(B) \equiv \frac{I_{\text{out}}(B)}{I_{\text{out}}^{(d)}(B)} , \tag{1.8a}$$

where the total intensity in reflection in the channel "out" is

$$I_{\text{out}}(B) = \left\langle \left| \frac{1}{\sqrt{2}} [E_{\text{out}}^{(d)}(B) + E_{\text{out}}^{(r)}(B)] \right|^2 \right\rangle_e$$

with $I_{\text{out}}^{(d)}(B) = \langle |E_{\text{out}}^{(d)}(B)|^2 \rangle_e$ and $I_{\text{out}}^{(r)}(B) = \langle |E_{\text{out}}^{(r)}(B)|^2 \rangle_e$ being the intensity of the channel "out" of the direct and reverse sequences, respectively, for an incidence in the channel "in." The symbol $\langle \cdots \rangle_e$ represents the ensemble average. Since $I_{\text{out}}^{(d)}(B) = I_{\text{out}}^{(r)}(B)$, we can write

$$\Xi_{\text{out,in}}(B) = 1 + \frac{\text{Re}[\langle E_{\text{out}}^{(d)}(B) E_{\text{out}}^{(r)}(B)^* \rangle_e]}{I_{\text{out}}^{(d)}(B)} . \tag{1.8b}$$

In the absence of a magnetic field there is no phase difference between the direct and the reverse path in the backscattering direction, and the enhancement factor is then equal to 2. Let us consider first $B=0$ and incident light polarized linearly along the x direction ($E_{0x} = E_0$ and $E_{0y} = 0$) and the detection is performed in this polarization channel (in=out=x). This is a typical same-channel configuration. From Eq. (1.6d), the diagonal elements of the direct and reverse sequences are the same, and consequently $E_x^{(d)}(0) = E_x^{(r)}(0) = j_{11}^{(n)} E_0$, which gives $\Xi_{x,x}(0) = 2$. Let us now consider the detection on the y channel, a typical opposite-channel configuration. The elements of the effective Jones matrix connecting $E_y^{(d)}(0)$ and $E_y^{(r)}(0)$ to E_0 are $j_{21}^{(n)}$ and $-j_{12}^{(n)}$, respectively. In this case $E_y^{(d)}(0) \neq E_y^{(r)}(0)$ and $\Xi_{x,x}(0) < 2$. For $E^{(d)}$ and $E^{(r)}$ completely incoherent, $\Xi = 1$.

For one dimension, the reverse sequence has the same effective Jones matrix as the direct one [Eq. (1.7a)]. The waves emerging from these sequences have the same polarization states even in the presence of a magnetic field. The enhancement factor is always 2. Obviously the time-reversal symmetry is broken but the backscattering cone is not affected. For two dimensions, the reverse sequence has an effective Jones matrix which is the transposed one [Eq. (1.7b)]. Hence the factor 2 does subsist (under a magnetic field) only for the same channel. In these two situations (one and two dimensions) and for the same polarization channel, the diagonal elements of the effective Jones matrix of the direct and reverse sequences are not modified by the transposition operation, giving rise to the factor 2. On the other hand, for the opposite channel, the factor 2 can be lowered for the two-dimensional system since the off-diagonal elements of the effective Jones matrix of the direct and reverse sequences are not the same. It is interesting to notice that the two-dimensional system in the presence of a magnetic field has the same features for the peak of the backscattering cone as the three-dimensional system without magnetic field.

In three dimensions, because of the inverse sign of **B** in Eq. (1.6d), the phase coherence that gives rise to the backscattering cone is partially destroyed by the action of the magnetic field as it was firstly noticed by Golubentsev[6] and MacKintosh and John.[7]

We stress that the reverse sequence is not strictly the time-reversed sequence because these sequences have different polarization states as input. These results are summarized in Table I.

D. The invariance of the opposite-helicity channel

So far, the general consideration of symmetry properties has not made reference to the ensemble average of the multiply scattered light. Let us now consider the same problem of the polarization transformation in the circular basis or left-right helicity basis, $E_\pm = E_x \pm jE_y$. In this basis the Jones matrix that connects the emerging to the incident field,

$$\begin{bmatrix} E_{n,+} \\ E_{n,-} \end{bmatrix} = \mathcal{J}(\hat{k}_1, \hat{k}_0) \begin{bmatrix} E_{n-1,+} \\ E_{n-1,-} \end{bmatrix}$$

is

TABLE I. Presence of the factor 2 in the backscattering cone as a function of the dimensionality and magnetic field.

Dimensionality	Magnetic field	Enhancement factor 2 (single scattering excluded) channels: xx	$++$	yx	$+-$	Time-reversal symmetry breaking
1	off	yes	none	none	yes	no
	on	yes	yes	yes	none	yes
2	off	yes	yes	none	no	no
	on	yes	no	no	no	yes
3	off	yes	yes	no	no	no
	on	no	no	no	no	yes

$$\mathcal{J}(\hat{k}_1,\hat{k}_0)=\frac{1}{2}\begin{bmatrix} j_{11}+j_{22}-j(j_{12}-j_{21}) & j_{11}-j_{22}+j(j_{12}+j_{21}) \\ j_{11}-j_{22}-j(j_{12}+j_{21}) & j_{11}+j_{22}+j(j_{12}-j_{21}) \end{bmatrix}, \tag{1.9}$$

where the j_{ij} are the matrix elements of the Jones matrix given by Eq. (1.2b). From the symmetry properties given previously in Eq. (1.4), it can be shown that $\mathcal{J}(-\hat{k}_0,-\hat{k}_1)=\mathcal{J}^{(t)}(\hat{k}_1,\hat{k}_0)$. On the other hand, the advantage of the circular basis is that the Faraday rotation is expressed by a diagonal matrix:

$$\mathcal{R}(\alpha)=\begin{bmatrix} e^{j\alpha} & 0 \\ 0 & e^{-j\alpha} \end{bmatrix}.$$

Consider a direct sequence of scattering in this basis using the quantum-mechanics notation

$$|\mathbf{E}^{(d)}\rangle=\mathcal{J}_{\mathrm{dir}}(\mathbf{B})|\sigma_0\rangle=\mathcal{R}(\alpha_n)\mathcal{J}(\hat{k}_n,\hat{k}_{n-1})\cdots\mathcal{R}(\alpha_1)\times\mathcal{J}(\hat{k}_1,\hat{k}_0)\mathcal{R}(\alpha_0)|\sigma_0\rangle .$$

By definition, the reverse sequence of scatterings is given by

$$|\mathbf{E}^{(r)}\rangle=\mathcal{J}_{\mathrm{rev}}(\mathbf{B})|\sigma_0\rangle =\mathcal{R}(-\alpha_0)\mathcal{J}(-\hat{k}_0,-\hat{k}_1)\cdots\mathcal{R}(-\alpha_{n-1})\times\mathcal{J}(-\hat{k}_{n-1},\hat{k}_0)\mathcal{R}(-\alpha_n)|\sigma_0\rangle ,$$

where we can write more simply $\mathcal{J}_{\mathrm{rev}}(\mathbf{B})=\mathcal{J}^{(t)}_{\mathrm{dir}}(-\mathbf{B})$.

For the evaluation of the enhancement factor defined in (1.8b) we must consider the interference term

$$\langle\sigma_n|\mathbf{E}^{(d)}\rangle\langle\mathbf{E}^{(r)}|\sigma_n\rangle =\langle\sigma_n|\mathcal{R}_n\mathcal{J}_{n,n-1}\mathcal{R}_{n-1}\cdots\mathcal{R}_1\mathcal{J}_{1,0}R_0|\sigma_0\rangle \times\langle\sigma_0|\mathcal{R}_n\mathcal{J}^{*}_{n,n-1}\mathcal{R}_{n-1}\cdots\mathcal{R}_1\mathcal{J}^{*}_{1,0}\mathcal{R}_0|\sigma_n\rangle , \tag{1.10}$$

where, for simplicity, $\mathcal{R}_n$ stands for $\mathcal{R}(\alpha_n)$, $\mathcal{J}_{n,n-1}=\mathcal{J}(\hat{k}_n,\hat{k}_{n-1})$, and $|\sigma_0\rangle$ and $|\sigma_n\rangle$ stand for the circular polarization eigenvectors for incident and emergent polarization. A selection rule can be established by considering the spectral representation of the matrix products,

$$\langle\sigma_n|\mathbf{E}^{(d)}\rangle\langle\mathbf{E}^{(r)}|\sigma_n\rangle=\sum_{\sigma_1,\ldots,\sigma_{n-1},\sigma_1',\ldots\sigma_{n-1}'}\langle\sigma_n|\mathcal{R}_n\mathcal{J}_{n,n-1}|\sigma_{n-1}\rangle\langle\sigma_{n-1}|\mathcal{R}_{n-1}\cdots|\sigma_1\rangle \times\langle\sigma_1|\mathcal{R}_1\mathcal{J}_{1,0}\mathcal{R}_0|\sigma_0\rangle\langle\sigma_0|\mathcal{R}_n\mathcal{J}^{*}_{n,n-1}|\sigma_{n-1}'\rangle \times\langle\sigma_{n-1}'|\mathcal{R}_{n-1}\cdots|\sigma_1'\rangle\langle\sigma_1'|\mathcal{R}_1\mathcal{J}^{*}_{1,0}\mathcal{R}_0|\sigma_n\rangle . \tag{1.11}$$

The selection rule originates from the double matrix element products. In the diffusion situation, the angles can be considered as independent and the average in ϕ makes the nonidentical matrix elements vanish:

$$\overline{\langle\sigma_i|\mathcal{R}_i\mathcal{J}_{i,i-1}|\sigma_{i-1}\rangle\langle\sigma_i'|\mathcal{R}_i\mathcal{J}^{*}_{i,i-1}|\sigma_{i-1}'\rangle} =\delta_{\sigma_i,\sigma_i'}\delta_{\sigma_{i-1},\sigma_{i-1}'}+\delta_{\sigma_i,-\sigma_i'}\delta_{\sigma_{i-1},-\sigma_{i-1}'} , \tag{1.12}$$

which leads to the helicity-preserving channel $\delta_{\sigma_i,\sigma_i'}$ and the opposite-helicity channel $\delta_{\sigma_i,-\sigma_i'}$. From this selection rule, one readily finds that in the helicity-preserving channel, for instance $++$, the phase variation is $\exp[-j\sum_{i=0}^{n}2\alpha_i\sigma_i]$, which leads to a damping of the enhancement factor as a function of $\mathbf{B}$. For the opposite channel $+-$, the Faraday rotations disappear by the rule $\delta_{\sigma,-\sigma'}$. This damping in the same polarization channel and the conservation in the opposite one were proposed by MacKintosh and John.[7]

It must be noticed that the ensemble average over the directions of the wave vectors $\hat{k}$ couples the orbital factors $\mathcal{J}_{n,n-1}$ with the Faraday rotations α_{n-1} and α_n. The decoupling assumption of the random-helicity model, which will be discussed in Sec. III, is not justified since α_n and $\mathcal{J}_{n,n-1}$ are related as shown by the spectral representation of the fields.

E. Rotatory power

In optically active media such as sugar, for instance, the two helicity states have different refractive indices: the rotation of the polarization states, in contrast to the Faraday rotation, is independent of the direction of propagation of the wave. In our notation, this is expressed by taking a rotation matrix $\mathcal{R}(\alpha)$ independent of $\hat{k}$, and therefore invariant in the reciprocal situation where $-\hat{k}$ is considered. It is then established in a straightforward way that the fields of the reverse sequences are given by the same relation as for $B=0$, so that $J_{\mathrm{rev}}(\alpha)=J^{(\mathrm{at})}_{\mathrm{dir}}(\alpha)$ in the rectangular basis or $J_{\mathrm{rev}}(\alpha)=J^{(t)}_{\mathrm{dir}}(\alpha)$ in the circular basis.

In reflection and in three dimensions, the backscattering cone is preserved in the same polarization channel (xx or $++$), while for the opposite channels (xy or $+-$) the rotation power of these optically active media decreases the enhancement factor, as noticed by MacKintosh and John.[7] This effect is indeed less spectacular than the Faraday effect, since in the opposite channels the cone is already attenuated for $B=0$.

F. Intensity correlation function

This correlation function is defined by

$$G_{xx}^{(2)}(B)\equiv\frac{\langle i_x(0)i_x(B)\rangle_e}{\langle i_x(0)\rangle_e\langle i_x(B)\rangle_e}-1\ , \tag{1.13}$$

where $i_x=|E_x|^2$. In the approximation of independent paths, the x component of the electric field coming out of a sample μ is $E_x^{(\mu)}=\sum_{\nu=1}^{N}E_{x,\nu}^{(\mu)}/\sqrt{N}$, where $E_{x,\nu}^{(\mu)}$ is the field of the νth sequence. The modulus $|E_{x,\nu}^{(\mu)}|$ is distributed according to the Rayleigh distribution and the phases $\phi_\nu^{(\mu)}$ are distributed uniformly in the interval $[0,2\pi]$. Let us consider the ensemble average of the term

$$\langle i_x(0)i_x(B)\rangle_e=\frac{1}{M}\sum_{\mu=1}^{M}\frac{1}{N^2}\sum_{\nu,\nu',\eta,\eta'=1}^{N}|E_{x,\nu}^{(\mu)}(0)||E_{x,\nu'}^{(\mu)}(B)||E_{x,\eta}^{(\mu)}(0)|^*|E_{x,\eta'}^{(\mu)}(B)|$$
$$\times\exp\{j[\phi_\nu^{(\mu)}(0)-\phi_{\nu'}^{(\mu)}(B)+\phi_\eta^{(\mu)}(0)-\phi_{\nu'}^{(\mu)}(B)]\}\ , \tag{1.14a}$$

where $M,N\gg 1$. Because of the uniform distribution of the phases, we must consider the two situations where the summations do not vanish: (i) $\nu=\nu'$ and $\eta=\eta'$ and (ii) $\nu=\eta'$ and $\nu'=\eta$, so that

$$\langle i_x(0)i_x(B)\rangle_e=\langle i_x(0)\rangle_e\langle i_x(B)\rangle_e+|\langle E_x(0)E_x^*(B)\rangle_e|^2\ , \tag{1.14b}$$

where now the average can be interpreted as if we had one sequence per sample but NM samples. This interpretation of the ensemble average is a justification for a Monte Carlo simulation.[5] Thus, the correlation function can be written as

$$G_{xx}^{(2)}(B)=\frac{|\langle E_x(0)E_x^*(B)\rangle_e|^2}{\langle i_x(0)\rangle_e\langle i_x(B)\rangle_e}\ . \tag{1.14c}$$

II. ONE-DIMENSIONAL ANISOTROPIC MULTIPLE SCATTERING

We consider a photon scattered in a chain aligned in the z direction along which a magnetic field B is applied. This system can be seen as a fiber or multiple-layered medium with incident light perpendicular to the planes (scatterers). In this chain, we are interested in the polarization properties originated by the vectorial nature of the electromagnetic field and we ignore all the amplitude effect due to the localization phenomenon, which affects the orbital part of the field functions. In one dimension, the electric field after $n-1$ scatterings is given by Eqs. (1.1) with $\phi_\kappa=0$ and θ_κ is still a random variable, but it can have only two values, either 0 in the forward scattering or π in the backward one. In the forward scattering the polarization is not changed and $J(\hat{k}_\kappa,\hat{k}_{\kappa-1})=S(1)I$. In the backward scattering the sign of the helicity of the wave is changed in the improper frame obtained by the transformation $x\to x$, $y\to -y$, and $z\to -z$. As mentioned previously, this reflection is described by the Pauli matrix σ_z: $J(\hat{k}_\kappa,\hat{k}_{\kappa-1})=S(-1)\sigma_z$. The algebra of the multiple scattering is simply achieved since $\sigma_z R(\alpha)=R(-\alpha)\sigma_z$. This simple commutation rule leads to an accumulation of the Faraday angles in a scattering sequence. For instance, the effective Jones matrix of a sequence of $n-1$ scatterings ending in either transmission or reflection can be written as

$$\begin{bmatrix} I \\ \sigma_z \end{bmatrix} R(\alpha_0+\alpha_1+\alpha_2+\cdots+\alpha_n)\ ,$$

where I corresponds to transmission and σ_z to reflection. For the one-dimensional model, we have that

$$\alpha_0+\alpha_1+\alpha_2+\cdots+\alpha_n=VBs_n\ ,$$

where s_n is the total length of the sequence. The electric field after $n-1$ scatterings is then written as

$$\begin{bmatrix} E_{nx} \\ E_{ny} \end{bmatrix}=\frac{-j\exp[-jks_n]}{k^n\prod_{\kappa=1}^{n}r_\kappa}[I\text{ or }\sigma_z]\times\begin{bmatrix}\cos(VBs_n) & -\sin(VBs_n)\\ \sin(VBs_n) & \cos(VBs_n)\end{bmatrix}\begin{bmatrix} E_{0x}\\ E_{0y}\end{bmatrix}\ , \tag{2.1}$$

As discussed previously, for reflection the reversed sequence is identical to the direct one. All the sequences with a given length s have the same Faraday rotation $\alpha=VBs$.

Let us first turn our attention to the average Stokes intensities I,Q,U,V:

$$\begin{bmatrix} I\\ Q\\ U\\ V\end{bmatrix}(B)=\left\langle\begin{bmatrix} i\\ q\\ u\\ v\end{bmatrix}(B)\right\rangle_s\propto\left\langle\begin{bmatrix}1 & 0 & 0 & 0\\ 0 & \cos(2VBs) & \sin(2VBs) & 0\\ 0 & \sin(2VBs) & \pm\cos(2VBs) & 0\\ 0 & 0 & 0 & \pm 1\end{bmatrix}\right\rangle_s\begin{bmatrix} i_0\\ q_0\\ u_0\\ v_0\end{bmatrix}\ , \tag{2.2}$$

where $\langle \cdots \rangle_s$ stands for the path-length average, and the Stokes intensities are $i=i_x+i_y$, $q=i_x-i_y$, $u=2\,\mathrm{Re}(E_xE_y^*)$, and $v=2\,\mathrm{Im}(E_xE_y^*)$ with $i=|E|^2$. The Mueller matrix is not diagonal because of the helical symmetry introduced by the magnetic field. If the incident polarization is a pure state, the Stokes sum rule $(i_0^2=q_0^2+u_0^2+v_0^2)$ can be applied. The polarization degree is then given by

$$P^2=\frac{Q^2+U^2+V^2}{I^2}=v_0'^2+[\langle\cos(2VBs)\rangle_s^2+\langle\sin(2VBs)\rangle_s^2](1-v_0'^2)\ , \tag{2.3}$$

where $v_0'=v_0/i_0$.

We notice that if $B=0$ the polarization degree equals 1: there is no depolarization. This is understood because the forward scattering does not change the polarization state and the backward scattering only changes the helicity. For incident circular polarization ($v_0=\pm i_0$), with a magnetic field on, there is no depolarization since the photon will leave the segment in a pure circular polarization state, with the same helicity as the incident one in transmission or in the opposite helicity in reflection. If the incident polarization is noncircular, because of the Faraday rotation, the outcoming polarization of each sequence can be altered for different path lengths, which produces a depolarization. The strongest one happens for linear incidence ($v_0=0$) and

$$P=\sqrt{\langle\cos(2VBs)\rangle_s^2+\langle\sin(2VBs)\rangle_s^2}\ .$$

In order to obtain the intensity correlation [Eq. (1.14c)], we first consider the field correlator $G^{(1)}$,

$$\begin{bmatrix} G_{xx}^{(1)} \\ G_{yy}^{(1)} \\ G_{xy}^{(1)} \\ G_{yx}^{(1)} \end{bmatrix}(B)=\left\langle \begin{bmatrix} E_x(0)E_x^*(B) \\ E_y(0)E_y^*(B) \\ E_x(0)E_y^*(B) \\ E_y(0)E_x^*(B) \end{bmatrix} \right\rangle_s \propto 1/2 \left\langle \begin{bmatrix} 2\cos(VBs) & 0 & -\sin(VBs) & -j\sin(VBs) \\ 0 & 2\cos(VBs) & \sin(VBs) & -j\sin(VBs) \\ 2\sin(VBs) & 0 & \cos(VBs) & j\cos(VBs) \\ 0 & -2\sin(VBs) & \cos(VBs) & -j\cos(VBs) \end{bmatrix} \right\rangle_s \begin{bmatrix} i_{0x} \\ i_{0y} \\ u_0 \\ v_0 \end{bmatrix} . \tag{2.4}$$

For the x component we obtain the intensity correlation function

$$G_{xx}^{(2)}(B)\frac{|G_{xx}^{(1)}|^2}{I_x(0)I_x(B)}=2\frac{\langle\cos(VBs)\rangle_s^2 i_{0x}+\langle\sin(VBs)\rangle_s^2 i_{0y}-\langle\cos(VBs)\rangle_s\langle\sin(VBs)\rangle_s u_0}{i_0+\langle\cos(2VBs)\rangle_s q_0-\langle\sin(2VBs)\rangle_s u_0} . \tag{2.5}$$

For linear incidence along the direction x ($i_{0x}=i_0=q_0$ and $u_0=0$) and for circular polarization ($i_{0x}=i_{0y}=i_0/2$ and $u_0=q_0=0$) one gets, respectively,

$$G_{xx}^{(2)}(B)=\frac{\langle\cos(VBs)\rangle_s^2}{\langle\cos^2(VBs)\rangle_s}$$

and

$$G_{xx}^{(2)}(B)=\langle\cos(VBs)\rangle_s^2+\langle\sin(VBs)\rangle_s^2\ . \tag{2.6}$$

The main result of this section is the complete correlation of the polarization, despite the random walk of photons in the chain, for given s. For the linear case, the numerator of $G_{xx}^{(2)}$ has an oscillatory behavior when B is varied. These oscillations are parametrized by the total length of the diffusion paths and, for one-dimensional systems, they are damped only through the path-length distribution $P(s)$.

In transmission, $P(s)$ is characterized by a dispersion, which can be pictured as a window along the s axis. Hence, for narrow distributions corresponding to thin slabs, oscillations arise from the average values of $\cos(VBs)$ and $\cos^2(VBs)$ inside this window. To be more explicit, in transmission, the Laplace transform of the path-length distribution gives

$$\int_L^\infty ds\,P(s)\exp(-VBs)\cong\frac{VBL}{\sinh(VBL)}$$

where the approximation holds for $L/\ell^*\gg 1$, where L is the chain length and the transport mean free path is $\ell^*=\ell/(1-\langle\cos\theta\rangle)$, with ℓ being the mean free path and $\langle\cos\theta\rangle=[S(1)+S(-1)]/2$. We have that $\langle\cos(VBs)\rangle_s=j_0(VBL)$,

$$\langle\cos^2(VBs)\rangle_s=\tfrac{1}{2}[1+j_0(2VBL)]\ ,$$

and

$$\langle\sin^2(VBs)\rangle_s=\tfrac{1}{2}[1-j_0(2VBL)]\ ,$$

where $j_0(x)=\sin(x)/x$. The intensity correlation function for the incident linear polarization is then given by

$$G_{xx}^{(2)}(B)=\frac{2j_0^2(VBL)}{1+j_0(2VBL)}\ , \tag{2.7}$$

which exhibits the oscillations. On the other hand, for this one-dimensional model the intensity correlation function for the incident circular polarization is always unity.

III. THREE-DIMENSIONAL RAYLEIGH MULTIPLE SCATTERING

A. The random-helicity model

1. Transmission

Let us recall the theoretical approach of MacKintosh and John[7] to the law of variation of $G_{xx}^{(2)}(B)$. Consider the isotropic scattering regime (Rayleigh regime): the wave vector $\hat{k}$ is randomized at the length scale ℓ, the mean free path. It is assumed that at the same length scale the polarization is randomized by a simple random process of helicity flip (of "Ising" type) in the circular wave representation. This is described by an external second random variable $\eta_\kappa = 1$ with equal probability, the index κ being the scattering label. The phase difference between right- and left-handed helicity is given by $\delta\phi_\kappa = \eta_\kappa \alpha_\kappa = \eta_\kappa V B \ell \cos\Omega_\kappa$, where Ω_κ, the angle between B and $\hat{k}_\kappa$, is uniformly distributed in the interval $[0,\pi]$. The phase difference is a random variable with zero mean value. For a given sequence, the total phase difference Φ between the circular states is

$$e^{j\Phi} = \prod_{\kappa=1}^{n} \exp(j\delta\phi_\kappa) = \exp\left[j \sum_{\kappa=1}^{n} \delta\phi_\kappa \right] .$$

Since the $\delta\phi_\kappa$ are assumed to be independent random variables of zero average, by virtue of the central limit theorem,

$$\langle \exp(j\Phi) \rangle_e = \exp(-n\langle \delta\phi^2 \rangle_e) = \exp(-n\langle \alpha^2 \rangle_e) .$$

Confining the scatterers in a slab of thickness L, we use the path-length distribution $P(s)$ from the diffusion theory ($L/\ell \gg 1$). In transmission, for $L/\ell \gg 1$ the transmitted light is completely depolarized, i.e., $\langle i_x(0) \rangle_e = \langle i_x(B) \rangle_e = \frac{1}{2}$. From Eq. (1.14c) one gets

$$G_{xx}^{(2)}(\xi) \propto \left[\int_L^\infty ds\, P(s) \exp\left[-\frac{s\langle \alpha^2 \rangle_e}{\ell} \right] \right]^2 \propto \left[\frac{\xi}{\sinh(\xi)} \right]^2 , \quad (3.1a)$$

where $\xi \propto L\sqrt{\langle \alpha^2 \rangle_e}/\ell = VBL$ for $\langle \alpha^2 \rangle_e \ll 1$. As usual, the mean free path disappears in the last expression. The reduced variable ξ couples exactly B and L through the factor BL. Consequently, this simple theory predicts a dependence of $G_{xx}^{(2)}$ on VBL as well as a Faraday correlation length proportional to B^{-1}.

2. Reflection

For reflection we are interested in the enhancement factor, so that we have to take into account the phase interference between the direct and reversed sequences. The phase difference induced by the Faraday rotation for the direct sequence is $E^{(d)} = e^{j\Phi} = \exp(j\sum_{\kappa=1}^{n}\delta\phi_\kappa)$. The total phase change induced by the Faraday rotation in the reverse sequence is

$$E^{(r)} = e^{-j\Phi} = \exp\left[-j \sum_{\kappa=1}^{n} \delta\phi_\kappa \right] ,$$

where the change $\mathbf{B}$ to $-\mathbf{B}$ [Eq. (1.6d)] has been done. The enhancement factor is then given by Eq. (1.8b):

$$\Xi(n) = 1 + \mathrm{Re}[\langle E^{(d)} E^{(r)*} \rangle_e] = 1 + \exp(-2n\langle \alpha^2 \rangle_e) .$$

Confining the scatterers in a slab of thickness L and using the path-length distribution from diffusion theory, we obtain

$$\Xi(B) - 1 \propto \int_\ell^\infty ds\, P(s) \exp\left[-\frac{2s\langle \alpha^2 \rangle_e}{\ell} \right] \propto \exp(-\sqrt{2} VB\ell) , \quad (3.1b)$$

where we have made use of $\langle \alpha^2 \rangle_e \ll 1$. The analogy of the Faraday enhancement factor as a function of VB with the enhancement factor of the coherent backscattering cone (as a function of the scattering angle) has been established by Lenke and Maret,[15] where they notice the difference of the slopes of these cones by a factor $\sqrt{2}$.

To conclude this brief summary, we emphasize that this simple random-helicity approach is not able to describe the persistence of the backscattering cone in the reduced-dimensionality systems. The anisotropy can be included in this simple model by changing the mean free path to the transport mean free path ℓ^*, as discussed in Ref. 14. This simple analysis assumes a randomization process for the polarization states in addition to the randomization of the wave vector $\hat{k}$. This is certainly a considerable approximation of the polarization problem which must be discussed carefully. For instance, in the one- and two-dimensional problems, the wave vector is randomized without any separate randomization of polarization (see Sec. II for the one-dimension case and Ref. 16 for the two-dimensional one).

B. Rayleigh scatterers

For the three-dimensional problem, we are not able to obtain a general analytical result beyond the simple results of Sec. I. In this section, we will develop a calculation in the Rayleigh regime while in the next section we will report numerical results of a Monte Carlo simulation for the Mie regime.

For Rayleigh scatterers $S_\perp(\cos\theta) \propto 1$ and $S_\parallel(\cos\theta) \propto \cos\theta$, and all the intermediate fields during the multiple scattering can be written in the laboratory frame (x,y,z) through the dipolar matrix ["Jones" matrix in the (x,y,z) frame]. For a sequence starting with $\hat{k}_0$ and ending with $\hat{k}_n$, the electric field is obtained from Eqs. (1.1). For pointlike scatterers it can be written as

$$\begin{bmatrix} E_{nx} \\ E_{ny} \\ 0 \end{bmatrix} \propto R(\alpha_n)\left\{\prod_{\kappa=1}^{n-1} T^{-1}(\hat{k}_\kappa)R(\alpha_\kappa)T(\hat{k}_\kappa)M(\hat{k}_\kappa)\right\} \times R(\alpha_0)\begin{bmatrix} E_{0x} \\ E_{0y} \\ 0 \end{bmatrix}, \tag{3.2a}$$

where the order in the product starts with the first term $\kappa=1$ in the right-hand side, with

$$R(\alpha)=\begin{bmatrix} \cos\alpha & -\sin\alpha & 0 \\ \sin\alpha & \cos\alpha & 0 \\ 0 & 0 & 1 \end{bmatrix},$$

$$M(\hat{k})=\begin{bmatrix} 1-k_x^2 & -k_xk_y & -k_xk_z \\ -k_xk_y & 1-k_y^2 & -k_yk_z \\ -k_xk_z & -k_yk_z & 1-k_z^2 \end{bmatrix}, \tag{3.2b}$$

and

$$T(\hat{k})=\begin{bmatrix} \cos\theta\cos\phi & \cos\theta\sin\phi & -\sin\theta \\ -\sin\phi & \cos\phi & 0 \\ \sin\theta\cos\phi & \sin\theta\sin\phi & \cos\theta \end{bmatrix},$$

where $\alpha=\varepsilon k_z$ with $\varepsilon=VB\ell$ (we assume that successive scatterers are separated by ℓ), $k_x=\sin\theta\cos\phi$, $k_y=\sin\theta\sin\phi$, and $k_z=\cos\theta$. We impose the condition that the Faraday rotation, described by the matrix $R(\alpha)$, occurs in the local frame throughout the action of the matrix T, which describes the change of frames. Using: $T^{-1}=T^{(t)}$, $M^2=M$, and $NM=MN=N$, one can write

$$M'=T^{-1}RTM=M\cos\alpha+N\sin\alpha$$

$$\text{with } N=\begin{bmatrix} 0 & -k_z & k_y \\ k_z & 0 & -k_x \\ -k_y & k_x & 0 \end{bmatrix}, \tag{3.2c}$$

where N, contrary to M, is an antisymmetric matrix. The obvious properties are $N^2=-M$ and $M'M=M'$. We notice that this matrix representation is equivalent to the recursive vectorial form,

$$E_\kappa=M'_\kappa E_{\kappa-1}=(\cos\alpha_\kappa\hat{k}_\kappa\wedge+\ \sin\alpha_\kappa)(\hat{k}_\kappa\wedge E_{\kappa-I}) .$$

The matrix M'_κ depends only on the scattering angles θ_κ and ϕ_κ which are the only random variables of the problem. Thus Eq. (3.2a) can be written as

$$\begin{bmatrix} E_{nx} \\ E_{ny} \\ 0 \end{bmatrix} \propto R(\alpha_n)\prod_{\kappa=1}^{n-1} M'(\hat{k}_\kappa)R(\alpha_0)\begin{bmatrix} E_{0x} \\ E_{0y} \\ 0 \end{bmatrix}, \tag{3.2d}$$

The multiple-scattering sequences are obtained by choosing the random variables $\hat{k}_0,\hat{k}_1,\ldots,\hat{k}_n$ as uniform and independent. The assumption of independence of $\hat{k}$ does not treat correctly the exit conditions for a slab, since the last scattering may be anywhere in space and not necessarily close to the boundary surface. Nevertheless, it is expected that for large values of n the correlation in the choice of $\hat{k}$ vanishes. This recursive method is a generalization, in order to include the Faraday effect, of the method employed by Akkermans *et al.*[17]

1. Stokes intensities and polarization degree

First, let us calculate the mean values of the Stokes intensities in the presence of a magnetic field. The nine elements of the coherence matrix are defined by $C_\kappa(\varepsilon)\equiv\langle E_\kappa(\varepsilon)E_\kappa^\dagger(\varepsilon)\rangle_e$, where $\langle\cdots\rangle_e$ is the ensemble average and $\dagger$ takes the transpose of $E_\kappa(\varepsilon)$ and conjugates it. The starting value is

$$C_0(\varepsilon)=R(\alpha_0)E_0(0)E_0^\dagger(0)R^{(t)}(\alpha_0) ,$$

and the rotation before the first scattering is then considered. The scatterings are independent of each other, allowing the recursion relation

$$C_\kappa(\varepsilon)=\langle M'_\kappa C_{\kappa-1}(\varepsilon)M'^{(t)}_\kappa\rangle ,$$

where now

$$\langle\cdots\rangle=\frac{1}{4\pi}\int_0^\pi d\theta_\kappa\sin\theta_\kappa\int_0^{2\pi}d\phi_\kappa\cdots .$$

Writing the elements of C_κ as a function of the elements of $C_{\kappa-1}$, we see that the integral in ϕ disconnects the elements in two sets, one with C_{xx}, C_{yy}, C_{zz}, C_{xy}, and C_{yx} and the other with C_{xz}, C_{zx}, C_{yx}, and C_{zy}. As we are interested in the outcoming field propagating along the z direction, only the x and y components are important; then we only consider the first set. This 5×5 matrix can be diagonalized into two 2×2 block matrices and one single element when transforming the C's into the Stokes intensities $I_\kappa=C_{xx,\kappa}+C_{yy,\kappa}$, $Q_\kappa=C_{xx,\kappa}-C_{yy,\kappa}$, $U_\kappa=C_{xy,\kappa}+C_{yx,\kappa}$, and $jV_\kappa=C_{xy,\kappa}-C_{yx,\kappa}$, and we obtain

$$\begin{bmatrix} I_\kappa \\ C_{zz,\kappa} \end{bmatrix}=\chi_1\begin{bmatrix} I_{\kappa-1} \\ C_{zz,\kappa-1} \end{bmatrix}, \quad \begin{bmatrix} Q_\kappa \\ U_\kappa \end{bmatrix}=\chi_2\begin{bmatrix} Q_{\kappa-1} \\ U_{\kappa-1} \end{bmatrix}, \text{ and } V_\kappa=\tfrac{1}{3}V_{\kappa-1} , \tag{3.3a}$$

where

$$\chi_I=\begin{bmatrix} c_{11} & 2c_{21} \\ c_{21} & c_{22} \end{bmatrix} \text{ and } \chi_2=\begin{bmatrix} c_{33} & c_{34} \\ -c_{34} & c_{33} \end{bmatrix}, \tag{3.3b}$$

with

$$c_{11}=\frac{7}{15}+\frac{1}{2\varepsilon^2}j_2(2\varepsilon),\quad c_{21}=\frac{1}{5}-\frac{1}{2\varepsilon^2}j_2(2\varepsilon) ,$$

$$c_{22}=\frac{4}{15}+\frac{1}{\varepsilon^2}j_2(2\varepsilon) ,$$

$$c_{33}=\frac{1}{15}+j_0(2\varepsilon)-\frac{1}{\varepsilon}j_1(2\varepsilon)+\frac{1}{4\varepsilon^2}j_2(2\varepsilon) , \tag{3.3c}$$

and

$$c_{34}=-j_1(2\varepsilon)+\frac{1}{2\varepsilon}j_2(2\varepsilon) ,$$

and $j_\kappa(\varepsilon)=\sqrt{(\pi/2\varepsilon)}J_{\kappa+1/2}(\varepsilon)$ is the spherical Bessel function and $J_\kappa(\varepsilon)$ the cylindrical one.

We are interested in considering $n-1$ scatterings. Thus we obtain for the $(n-1)$th power of the 2×2 matrices χ_1 and χ_2

$$\chi_1^{n-1}=\frac{1}{3}\frac{1}{2^{n-1}}\begin{bmatrix} 2(\frac{4}{3})^{n-1}+\gamma^{n-1} & 2[(\frac{4}{3})^{n-1}-\gamma^{n-1}] \\ (\frac{4}{3})^{n-1}-\gamma^{n-1} & (\frac{4}{3})^{n-1}+2\gamma^{n-1}\end{bmatrix}, \tag{3.4a}$$

and

$$\chi_2^{n-1}=\begin{bmatrix} \mathrm{Re}(\gamma'^{n-1}) & \mathrm{Im}(\gamma'^{n-1}) \\ -\mathrm{Im}(\gamma'^{n-1}) & \mathrm{Re}(\gamma'^{n-1})\end{bmatrix}, \tag{3.4b}$$

where $\gamma=\frac{2}{15}+(3/\varepsilon^2)j_2(2\varepsilon)$ and $\gamma'=c_{33}+jc_{34}=|\gamma'|e^{j\Phi}$, with $|\gamma'|=\sqrt{c_{33}^2+c_{34}^2}$ and $\Phi=\arctan(c_{34}/c_{33})$. These complicated expressions can be simplified for the case of (i) weak magnetic field ($\varepsilon\ll 1$): $\gamma=\frac{14}{15}-\frac{24}{105}\varepsilon^2$ and $\gamma'=\frac{7}{15}-\frac{44}{105}\varepsilon^2-j\frac{8}{15}\varepsilon$, and (ii) strong magnetic field ($\varepsilon\gg 1$): $\gamma=\frac{2}{5}$ and $\gamma'=\frac{1}{15}$. We notice that γ' is a complex variable for weak field which becomes asymptotically a real variable for a strong magnetic field.

Let us now consider the exit conditions: normal incidence and emergence in transmission and reflection. For the incidence, the first Faraday rotation is along the z axis so that the Stokes intensities are $I_0=i_0$,

$$Q_0=\cos(2\varepsilon_0)q_0-\sin(2\varepsilon_0)u_0\ ,$$
$$U_0=\sin(2\varepsilon_0)q_0+\cos(2\varepsilon_0)u_0\ ,$$

and $V_0=v_0$. The last Faraday rotation is also supposed to be along the z axis, with k_z taking two values, $+1$ in transmission and -1 in reflection. This leads to the relations $I_n=I_{n-1}$,

$$Q_n=\cos(2\varepsilon_n)Q_{n-1}-\sin(2\varepsilon_n)U_{n-1}\ ,$$
$$U_n=\sin(2\varepsilon_n)Q_{n-1}+\cos(2\varepsilon_n)U_{n-1}\ ,$$

and $V_n=V_{n-1}$. In this way we obtain (without approximation) the Mueller matrix with a magnetic field:

$$\begin{bmatrix} I_n\\ Q_n\\ U_n\\ V_n\end{bmatrix}(\varepsilon)=\tfrac{1}{3}(\tfrac{1}{2})^{n-1}[2(\tfrac{4}{3})^{n-1}+\gamma^{n-1}]\begin{bmatrix} 1 & 0 & 0 & 0\\ 0 & P_L^{(n)}\cos[(n-1)\Phi-2(\varepsilon_0+\varepsilon_n)] & P_L^{(n)}\sin[(n-1)\Phi-2(\varepsilon_0+\varepsilon_n)] & 0\\ 0 & P_L^{(n)}\sin[(n-1)\Phi-2(\varepsilon_0+\varepsilon_n)] & \pm P_L^{(n)}\cos[(n-1)\Phi-2(\varepsilon_0+\varepsilon_n)] & 0\\ 0 & 0 & 0 & \pm P_C^{(n)}\end{bmatrix}\begin{bmatrix} i_0\\ q_0\\ u_0\\ v_0\end{bmatrix}, \tag{3.5a}$$

where

$$P_L^{(n)}=\frac{3(2|\gamma'|)^{n-1}}{2(\frac{4}{3})^{n-1}+\gamma^{n-1}} \tag{3.5b}$$

is the polarization degree $[P^{(n)}(\varepsilon)=\sqrt{(Q_n^2+U_n^2+V_n^2)/I_n^2}]$ for *linear* incident polarization in x ($q_0=i_0$ and $u_0=v_0=0$) and

$$P_C^{(n)}=\frac{3(\frac{2}{3})^{n-1}}{2(\frac{4}{3})^{n-1}+\gamma^{n-1}} \tag{3.5c}$$

is the polarization degree for *circular* incidence ($v_0=\pm i_0$ and $q_0=u_0=0$). For $B=0$, we find the values calculated by Akkermans *et al.*:[17]

$$\begin{bmatrix} I_n\\ Q_n\\ U_n\\ V_n\end{bmatrix}(0)=\begin{bmatrix} \frac{1}{3}[2(\frac{2}{3})^{n-1}+(\frac{7}{15})^{n-1}] & 0 & 0 & 0\\ 0 & (\frac{7}{15})^{n-1} & 0 & 0\\ 0 & 0 & \pm(\frac{7}{15})^{n-1} & 0\\ 0 & 0 & 0 & \pm(\frac{1}{3})^{n-1}\end{bmatrix}\begin{bmatrix} i_0\\ q_0\\ u_0\\ v_0\end{bmatrix}. \tag{3.5d}$$

The symmetry of this matrix is discussed in Ref. 4 and the polarization degree for linear and circular incident polarization is discussed in Ref. 5.

We see that the Mueller matrix of Eq. (3.5a) has the same structure as the one-dimension matrix [Eq. (2.2)]. Simpler expressions can be obtained in the diffusion regime ($n\gg 1$) under weak ($\varepsilon\ll 1$) and strong ($\varepsilon\gg 1$) magnetic field. For weak magnetic field we have that

$$\begin{bmatrix} I_n\\ Q_n\\ U_n\\ V_n\end{bmatrix}(\varepsilon)=(\tfrac{2}{3})^n\begin{bmatrix} 1 & 0 & 0 & 0\\ 0 & P_L^{(n)}\cos(\frac{8}{7}n\varepsilon) & -P_L^{(n)}\sin(\frac{8}{7}n\varepsilon) & 0\\ 0 & -P_L^{(n)}\sin(\frac{8}{7}n\varepsilon) & \pm P_L^{(n)}\cos(\frac{8}{7}n\varepsilon) & 0\\ 0 & 0 & 0 & \pm P_C^{(n)}\end{bmatrix}\begin{bmatrix} i_0\\ q_0\\ u_0\\ v_0\end{bmatrix}, \tag{3.6a}$$

where we notice that, despite the small value of ε, the product $n\varepsilon$ can be much larger than unity. The polarization degrees are given by

$$P_L^{(n)}(\varepsilon)=P_L^{(n)}(0)\exp\left[-\frac{436}{1575}\varepsilon^2 n\right]$$

and (3.6b)

$$P_C^{(n)}(\varepsilon)=P_C^{(n)}(0)=(\tfrac{1}{2})^n ,$$

with $P_L^{(n)}(0)=(\frac{7}{10})^n$. For Rayleigh scatterers, the magnetic field does not modify the depolarization rate for the incident circular polarization. On the other hand, the magnetic field induces a faster decay for incident linear polarization, through the ε^2 term. For strong magnetic field, the Mueller matrix is

$$\begin{bmatrix} I_n \\ Q_n \\ U_n \\ V_n \end{bmatrix}(\varepsilon)=(\tfrac{2}{3})^n \begin{bmatrix} 1 & 0 & 0 & 0 \\ 0 & P_L^{(n)}\cos[2(\varepsilon_0+\varepsilon_n)] & -P_L^{(n)}\sin[2(\varepsilon_0+\varepsilon_n)] & 0 \\ 0 & -P_L^{(n)}\sin[2(\varepsilon_0+\varepsilon_n)] & \pm P_L^{(n)}\cos[2(\varepsilon_0+\varepsilon_n)] & 0 \\ 0 & 0 & 0 & \pm P_C^{(n)} \end{bmatrix} \begin{bmatrix} i_0 \\ q_0 \\ u_0 \\ v_0 \end{bmatrix} . \tag{3.6c}$$

where the angle $2(\varepsilon_0+\varepsilon_n)$ corresponds to the Faraday rotations before the first scattering and after the last one. The polarization degrees are given by

$$P_L^{(n)}=\tfrac{3}{4}(\tfrac{1}{10})^n \text{ and } P_C^{(n)}=\tfrac{3}{2}(\tfrac{1}{2})^n . \tag{3.6d}$$

In this case the depolarization rate is faster for the incident linear polarization state than for the circular one, in contrast to the zero-field situation.

2. *Destruction of the backscattering enhancement*

For reflection, we must consider the reverse sequences. These sequences are obtained by taking $\hat{k}\to-\hat{k}$ and consequently $\alpha\to-\alpha$ and reversing the order of the sequence. The electric field of the direct sequence is given by Eq. (3.2d) and the electric field of the reverse one is given by

$$\begin{bmatrix} E_{nx} \\ E_{ny} \\ 0 \end{bmatrix} \propto R(-\alpha_0)\prod_{\kappa=n-1}^{1} M'(-\hat{k}_\kappa)R(-\alpha_n)\begin{bmatrix} E_{0x} \\ E_{0y} \\ 0 \end{bmatrix} , \tag{3.7}$$

where the order of the product has been reversed. The field emerging from the slab in reflection is the sum of the direct and the reversed one.

We will consider the xx configuration, i.e., only the x component of the emerging electric field for the sequences with n scatterings. The enhancement factor is given by Eq. (1.8):

$$\Xi_{xx}(\varepsilon)=\frac{I_x(\varepsilon)}{I_x^{(d)}(\varepsilon)}=1+\frac{\mathrm{Re}[\Gamma_{xx}(\varepsilon)]}{I_x^{(d)}(\varepsilon)} , \tag{3.8a}$$

with

$$I_x^{(d)}(\varepsilon)=I_x^{(r)}(\varepsilon)=\frac{I+Q}{2}$$

and

$$\Gamma_{xx}^{(n)}(\varepsilon)=\langle E_x^{(d)}(\varepsilon)E_x^{(r)\dagger}(\varepsilon)\rangle=[100]\langle X_n(\varepsilon)\rangle\begin{bmatrix}1\\0\\0\end{bmatrix}$$
$$=\langle X_{xx,n}(\varepsilon)\rangle i_0 . \tag{3.8b}$$

We also ignore the first and last Faraday rotation, $\alpha_0=\alpha_n=0$. In this case, we can write

$$\langle X_{n-1}(\varepsilon)\rangle=M'_1M'_2\cdots M'_{n-1}(\varepsilon)\begin{bmatrix}1\\0\\0\end{bmatrix}[100]\,M_1'^{(t)}M_2'^{(t)}\cdots M_{n-1}'^{(t)}$$
$$=[M_{n-1}'^{(t)}\cdots M_2'^{(t)}M_1'^{(t)}]^{(t)}\begin{bmatrix}1\\0\\0\end{bmatrix}[100]\,M_1'^{(t)}M_2'^{(t)}\cdots M_{n-1}'^{(t)}$$
$$=\langle M_{n-1}'^{(t)}(\varepsilon)\langle X_{n-2}(\varepsilon)\rangle M_{n-1}'^{(t)}(\varepsilon)\rangle . \tag{3.8c}$$

Writing the elements of X_n as a function of the elements of X_{n-1}, we see that the average in ϕ disconnects these elements in two sets, one with X_{xx}, X_{yy}, X_{zz}, X_{xy}, and X_{yx} and the other X_{xz}, X_{zx}, X_{yz}, and X_{zy}. As we are interested in the x component propagating along the z axis, we will consider only the fist set. Performing the transformation $X_i=X_{xx}+X_{yy}$, $X_q=X_{xx}-X_{yy}$, $X_u=X_{xy}+X_{yx}$, and $X_v=X_{xy}-X_{yx}$, the 5×5 matrix can be rewritten in blocks with a 3×3 matrix and two degenerate eigenvalues,

$$\begin{bmatrix} X_{i,n-1} \\ X_{v,n-1} \\ X_{zz,n-1} \end{bmatrix}(\varepsilon)=\chi_3^{n-1}(\varepsilon)\begin{bmatrix} X_{i,0} \\ X_{v,0} \\ X_{zz,0} \end{bmatrix},$$

$$X_{q,n-1}(\varepsilon)=\tilde{a}_2^{n-1}(\varepsilon)X_{q,0},$$

and (3.9a)

$$X_{u,n-1}(\varepsilon)=\tilde{a}_2^{n-1}(\varepsilon)X_{u,0};$$

where

$$\chi_3(\varepsilon)=\begin{bmatrix} x_{11} & x_{12} & 2x_{13} \\ -x_{12} & x_{22} & -2x_{23} \\ x_{13} & x_{23} & x_{33} \end{bmatrix}$$

and (3.9b)

$$\tilde{a}_2(\varepsilon)=\frac{2}{5}+\frac{1}{4\varepsilon^2}j_2(2\varepsilon).$$

Here,

$$x_{11}=\frac{2}{15}+j_0(2\varepsilon)-\frac{1}{\varepsilon}j_1(2\varepsilon)+\frac{1}{2\varepsilon^2}j_2(2\varepsilon),$$

$$x_{12}=-j_1(2\varepsilon)+\frac{1}{2\varepsilon}j_2(2\varepsilon),$$

$$x_{13}=-\frac{2}{15}+\frac{1}{2\varepsilon}j_1(2\varepsilon)-\frac{1}{2\varepsilon^2}j_2(2\varepsilon), \quad (3.9c)$$

$$x_{22}=j_0(2\varepsilon)-\frac{1}{\varepsilon}j_1(2\varepsilon),$$

$$x_{23}=-\frac{1}{2\varepsilon}j_2(2\varepsilon),\quad x_{33}=\frac{4}{15}+\frac{1}{\varepsilon^2}j_2(2\varepsilon).$$

Let us now consider the eigenvalues of χ_3. For small values of ε we have $\lambda_1(\varepsilon)\cong\frac{2}{3}(1-2\varepsilon^2)$, $\lambda_2(\varepsilon)\cong\frac{1}{3}(1+2\varepsilon^2)$, and $\lambda_3(\varepsilon)\cong\frac{7}{15}(1-\frac{8}{15}\varepsilon^2)$. For large values of ε, the Bessel functions are very small, so that $\lambda_1(\varepsilon)\cong\frac{2}{5}$, $\lambda_2(\varepsilon)=\lambda_3(\varepsilon)\cong 0$. Since in both limiting cases $\lambda_1^n(\varepsilon)$ is much greater than $\lambda_2^n(\varepsilon)$ and $\lambda_3^n(\varepsilon)$, in the diffusion regime ($n\gg 1$) we can write

$$X_{i,n}(\varepsilon)\cong\lambda_1^n(\varepsilon)X_{i,0}. \quad (3.10)$$

Similarly, for small values of ε, $\tilde{a}_2(\varepsilon)\cong\frac{7}{15}(1-\frac{2}{49}\varepsilon^2)$, and for large values of ε, $\tilde{a}_2(\varepsilon)=\frac{2}{5}$. Thus one gets

$$X_{xx,n}=\frac{X_{i,n}+X_{q,n}}{2}=\frac{\lambda_1^n+\tilde{a}_2^n}{2}i_0. \quad (3.11a)$$

The enhancement factor is obtained from Eqs. (3.8a) and (3.8b):

$$\Xi_{xx,n}(\varepsilon)=1+\frac{X_{xx,n}(\varepsilon)}{I_{x,n}^{(d)}(\varepsilon)}=1+\frac{2X_{xx,n}(\varepsilon)}{I_n(\varepsilon)+Q_n(\varepsilon)}, \quad (3.11b)$$

where $I_n(\varepsilon)$ and $Q_n(\varepsilon)$ are the Stokes intensities given by Eq. (3.6a) in the limit of small values of ε and by Eq. (3.6c) in the limit of large values of ε. For incident linear polarized light along the x axis, the incident Stokes intensities are $q_0=i_0$ and $u_0=v_0=0$. For $\varepsilon\ll 1$, $\lambda_1(\varepsilon)>\tilde{a}_2$, so that for $n\gg 1$ the leading term is $\lambda_1(\varepsilon)$. The enhancement factor is then given by

$$\Xi_{xx,n}\cong 1+\exp(-2\varepsilon^2 n), \quad (3.12a)$$

which shows an exponential decrease as a function of $2\varepsilon^2 n$. In this way, we find the same result predicted by the random-helicity model. For $\varepsilon\gg 1$, the enhancement factor goes to 1 as

$$\Xi_{xx,n}(\varepsilon)-1\cong 2(\tfrac{3}{5})^n. \quad (3.12b)$$

For strong magnetic fields the enhancement factor does not converge to 1, since it depends on the number of scatterings n. In the backscattering geometry the most frequent paths are short, so that n may be small. The Faraday cone is destroyed exponentially as a function of the scattering number n with a characteristic decay $1/2\varepsilon^2$.

3. Correlation function

Let us now turn our attention to the product $G_\kappa(\varepsilon)=\langle E_\kappa(0)E_\kappa^\dagger(\varepsilon)\rangle_e$ which gives the field correlations. The generalized cohence matrix $G(\varepsilon)$ is obtained by the product

$$G_\kappa(\varepsilon)\langle M_k M_{k-1}\cdots M_1 G_0(\varepsilon)M_1^{\prime(t)}M_2^{\prime(t)}\cdots M_k^{\prime(t)}\rangle.$$

The initial value is defined as $G_0(\varepsilon)=E_0(0)E_0^\dagger(0)R^{(t)}(\alpha_0)$. As previously, we will ignore the first and the last Faraday rotation of the sequence. Assuming that the scatterings are independent of each other, one can use the recursion method,

$$G_\kappa(\varepsilon)=\langle M_\kappa G_{\kappa-1}(\varepsilon)M_\kappa^{\prime(t)}\rangle. \quad (3.13)$$

Writing the elements of G_κ as a function of the elements of $G_{\kappa-1}$, we see that, after averaging in ϕ, the values of G_{xx}, G_{yy}, G_{zz}, G_{xy}, and G_{yx} are independent of the values G_{xz}, G_{zx}, G_{yz}, and G_{zy}. As we are interested in the outcoming field, only the x and y components are important; we will thus consider the first set. We observe that G_{xy} is not the complex conjugate of G_{yx}. Changing the variables $G_i=G_{xx}+G_{yy}$, $G_q=G_{xx}-G_{yy}$, $G_u=G_{xy}+G_{xy}$, and $G_v=G_{xy}-G_{xy}$, we obtain a reduction of the 5×5 matrix in terms of a 2×2 matrix Γ_1 and a 3×3 matrix Γ_2:

$$\begin{bmatrix} G_{q,n-1} \\ G_{u,n-1} \end{bmatrix}=\Gamma_1^{n-1}(\varepsilon)\begin{bmatrix} G_{q,0} \\ G_{u,0} \end{bmatrix}$$

and (3.14a)

$$\begin{bmatrix} G_{i,n-1} \\ G_{v,n-1} \\ G_{zz,n-1} \end{bmatrix}=\Gamma_2^{n-1}(\varepsilon)\begin{bmatrix} G_{i,0} \\ G_{v,0} \\ G_{zz,0} \end{bmatrix},$$

with

$$\Gamma_1(\varepsilon)=\begin{bmatrix} g_{11} & g_{12} \\ -g_{12} & g_{11} \end{bmatrix}$$

and (3.14b)

$$\Gamma_2(\varepsilon)=\begin{bmatrix} g_{33} & g_{12} & 2g_{53} \\ -g_{12} & g_{44} & -2g_{54} \\ g_{53} & g_{54} & g_{55} \end{bmatrix},$$

and

$$\begin{aligned} g_{11}&=j_0(\varepsilon)-\frac{2}{\varepsilon}j_1(\varepsilon)+\frac{2}{\varepsilon^2}j_2(\varepsilon), \\ g_{12}&=-j_1(\varepsilon)+\frac{1}{\varepsilon}j_2(\varepsilon), \\ g_{33}&=j_0(\varepsilon)-\frac{2}{\varepsilon}j_1(\varepsilon)+\frac{4}{\varepsilon^2}j_2(\varepsilon), \\ g_{44}&=j_0(\varepsilon)-\frac{2}{\varepsilon}j_1(\varepsilon), \\ g_{53}&=j_1(\varepsilon)-\frac{4}{\varepsilon^2}j_2(\varepsilon), \\ g_{54}&=-\frac{1}{\varepsilon}j_2(\varepsilon),\quad g_{55}=\frac{8}{\varepsilon^2}j_2(\varepsilon). \end{aligned} \tag{3.14c}$$

For $n-1$ scatterings, we have

$$\Gamma_1^{n-1}=\begin{bmatrix} \mathrm{Re}(\gamma'') & \mathrm{Im}(\gamma'') \\ -\mathrm{Im}(\gamma'') & \mathrm{Re}(\gamma'') \end{bmatrix}$$

$$\text{with } \gamma''=(g_{11}+jg_{12})^{n-1}. \tag{3.15a}$$

For $\varepsilon \ll 1$ and for $n>>1$, we can write $\gamma''=(\frac{7}{15})^n\exp(-j\frac{4}{7}\varepsilon n)$ and Γ_1^{n-1} becomes a rotation matrix damped with a factor $(\frac{7}{15})^n$:

$$\Gamma_1^{n-1}\cong(\tfrac{7}{15})^n\begin{bmatrix} \cos(\frac{4}{7}\varepsilon n) & -\sin(\frac{4}{7}\varepsilon n) \\ \sin(\frac{4}{7}\varepsilon n) & \cos(\frac{4}{7}\varepsilon n) \end{bmatrix}. \tag{3.15b}$$

Now consider the 3×3 matrix Γ_2. For small values of ε, the eigenvalues of Γ_2 are $\lambda_1(\varepsilon)=\frac{2}{3}(1-\frac{1}{2}\varepsilon^2)$, $\lambda_2(\varepsilon)=\frac{1}{3}(1+\frac{1}{2}\varepsilon^2)$, and $\lambda_3(\varepsilon)=\frac{7}{15}(1-\frac{19}{98}\varepsilon^2)$. In the diffusion regime $n\gg1$, the leading term is given by the largest eigenvalue, which is $\lambda_1(\varepsilon)$, so that $G_{i,n}(\varepsilon)\cong\lambda_1^n(\varepsilon)G_{i,0}$. In order to calculate the intensity correlation function, we have to obtain $G_{xx}(\varepsilon)$ for incident light linearly polarized along the x direction and circularly polarized. In both cases, $G_{u,0}=0$ in Eq. (3.14a), which leads to

$$\begin{aligned} G_{xx}(\varepsilon)&=\langle E_x(0)E_x(\varepsilon)^\dagger\rangle_e \\ &=\frac{G_i(\varepsilon)+G_q(\varepsilon)}{2} \\ &\cong\tfrac{1}{2}[\lambda_1^n(\varepsilon)G_{i,0}+(\tfrac{7}{15})^n\cos(\tfrac{4}{7}\varepsilon n)G_{q,0}]. \end{aligned} \tag{3.16a}$$

Let us first consider an incident circular polarization. In this case $G_{q,0}=0$, so that

$$|G_{xx}(\varepsilon)|^2=\tfrac{1}{4}\lambda_1^{2n}(\varepsilon)i_0^2=\tfrac{1}{4}(\tfrac{2}{3})^{2n}\exp(-\varepsilon^2 n)i_0^2. \tag{3.16b}$$

The Stokes intensity along the x direction is given by Eq. (3.6a) and reads $I_x(\varepsilon)\cong\frac{1}{2}(\frac{2}{3})^n i_0$, so that the intensity correlation function is given by

$$G_{xx}^{(2)}(\varepsilon)=\frac{|G_{xx}(\varepsilon)|^2}{I_x(0)I_x(\varepsilon)}\cong\exp(-\varepsilon^2 n). \tag{3.16c}$$

Let us now consider incident linear light polarized along the x direction. In this case $G_{q,0}=G_{i,0}=i_0$, so that

$$\begin{aligned} G_{xx}^{(2)}(\varepsilon)&=\frac{|G_{xx}(\varepsilon)|^2}{I_x(0)I_x(\varepsilon)} \\ &\cong\exp(-\varepsilon^2 n)[1+2(\tfrac{7}{10})^n\exp(\varepsilon^2 n/2)\cos(\tfrac{4}{7}\varepsilon n)]. \end{aligned} \tag{3.16d}$$

For $\varepsilon^2 n\ll1$, we cannot make any distinction between the incident linear and circular polarization since both correlation functions decay as $\exp(-\varepsilon^2 n)$. This is a result obtained by the random-helicity model. This fact was observed experimentally by Erbacher, Lenke, and Maret.[8] Nevertheless, the correlation function for incident linear and circular polarization has different behaviors for larger values of $\varepsilon^2 n$. For circular polarization it keeps decaying as $\exp(-\varepsilon^2 n)$, but for the incident linear polarization, this function is only the envelope of an oscillating function with period of $\varepsilon n=7\pi/2$. This kind of oscillation has also been observed in a Monte Carlo simulation.[9]

IV. MONTE CARLO SIMULATION

A. Algorithm

To simulate sequences of Mie scatterings in a slab of length L under a magnetic field B, we have included the Faraday rotations between the scatterers in the Monte Carlo code we have developed to study the statistics of the polarization.[5] In this code, the Mie coefficients and scattering amplitudes $S_\parallel(\cos\theta)$ and $S_\perp(\cos\theta)$ have been obtained as described in Ref. 18 using the Lentz algorithm.[19] The Jones matrix of each Mie scattering contains the Faraday rotation due to the magnetic field. The effect of the magnetic field inside the scatterers is ignored. These matrices are calculated using the Chandrasekhar-Sekera representation.[11,12]

In the slab, the photon history starts at the origin of the laboratory (lab) frame (x,y,z). It propagates along the z axis until $z'>0$. This distance is generated following the exponential distribution $\exp(-r/\ell)/\ell$. The distance $\ell=1/(\rho\sigma_t)$ is the mean free path, where ρ is the concentration of spheres and σ_t is the total cross section (we do not consider the effects of absorption). If $z'>L$, the photon leaves the slab without being scattered and the Faraday rotation inside the slab is taken into account. On the other hand, if $0<z'<L$, the Faraday rotation is taken into account for this segment and a sphere of radius a is supposed to be present at this position. A local coordinate system is considered so that $\hat{x}_1=\hat{x}$, $\hat{y}_1=\hat{y}$, and $\hat{z}_1=\hat{z}$. In this local frame the scattering angles θ_1 and ϕ_1 are generated by the Mie distribution and a new distance r_1 is generated by the exponential distribution. This new position (θ_1,ϕ_1,r_1) corresponds to a new scattering and its coordinates are then calculated in the lab frame (x_1,y_1,z_1). If $z_1>L$, the photon is transmitted and if

$z_1 < 0$, the phonon is reflected. In both cases, the photon leaves the slab perpendicularly to the walls, suffering one collision, and the Faraday rotation is taken into account for this segment. If the photon does not escape the slab, the Faraday rotation corresponding to this segment is considered as well as a new local coordinated system, $\hat{x}_2=\hat{\theta}_1$, $\hat{y}_2=\hat{\phi}_1$, and $\hat{z}_2=\hat{k}_1$. The scattering angles are chosen following the Mie distribution and a new distance is generated in this new local frame. This position is calculated in the lab frame and this process is repeated successively until a sphere lies outside the slab. When the exit condition is satisfied, the last scattering is taken back and the photon is forced to be scattered in the direction $\hat{\theta}'$ and $\hat{\phi}'$ in the last local frame. These last scattering angles are not random, but calculated so that the photon escapes perpendicularly to the plane of the slab. In transmission, the multiply scattered Jones matrix is calculated in the lab frame $(\hat{\theta}'=\hat{x},\hat{\phi}'=\hat{y},\hat{k}'=\hat{z})$, but in reflection, it is calculated in the frame $(\hat{\theta}'=\hat{x}, \hat{\phi}'=-\hat{y},\hat{k}'=-\hat{z})$, which is an improper rotation of the lab frame. A weight (the probability for a photon to be scattered with the angles θ' and ϕ') is then assigned to each sequence. The reverse sequence is calculated so that, if the phonon quits the slab in reflection, the Jones matrix of the reverse sequence is considered. The Mueller matrices are then calculated and the averages are performed. In this way we obtain the enhancement factor and the intensity correlations as a function of the magnetic field and slab length.

An important step of the method resides in the choice of the scattering angles θ and ϕ. We emphasize that the complete Mie distribution is not separable. Even worse, it is parametrized by the incident field. Generating this distribution numerically, by the rejection method, is very time consuming. For large spheres, the distribution takes a simpler form. It is independent of both ϕ and the incident field. Therefore, the angle ϕ can be chosen from a uniform distribution and the angle θ is given by the approximate large-sphere Mie distribution

$$[|S_{\parallel}(\cos\theta)|^2+|S_{\perp}(\cos\theta)|^2]/(2\sigma_s) ,$$

where σ_s is the scattering cross section. This simplification has already been used in previous simulations.[20–22] In this case, the angle θ can be generated by the cumulative function (the integral of the large-sphere Mie distribution). This method is very efficient, since a single random number is needed for each $\cos\theta$. The values of the cumulative function can be tabulated as well as the values of the scattering amplitudes. The tables are divided into 180 intervals of $\cos\theta$ and data are obtained from these tables by linear interpolation.

We stress that the fields are propagated in our program, and not the intensities. The selection rule [Eq. (1.12)] which assures the invariance of the opposite circular channel is not used in the Monte Carlo code but it comes out as a result.

B. Results

We have considered incident circular and linearly polarized light along the x axis with a wavelength in the vacuum $\lambda_{\text{vac}}=0.4579$ μm. The Verdet constant of the medium is $V=157.1$ rad/mT and its refraction index $n_m=1.69$. The spheres have a radius $a=0.1$ μm and a refraction index $n_s=1.45$ and are diluted, representing 1% of the volume. This leads to a size parameter $ka=2\pi n_m a/\lambda_{\text{vac}}=2.32$. The magnetic field is applied along the z axis and we have considered at least 10 000 sequences for each slab thickness.

From the Mie regime ($ka=2.32$ and $m=n_s/n_m=0.858$) we obtain a total scattering cross section $\sigma_t=4.41\times10^{-3}$ μm^2, $\ell=1/(\rho\sigma_t)=0.0951$ mm, the mean value of the cosine of the scattering angle is $\langle\cos\theta\rangle=0.669$ leading to a transport mean free path $\ell^*/\ell=1/(1-\langle\cos\theta\rangle)=3.02$, and the Ioffe-Regel parameter $k\ell=2205$. These values correspond to the experimental situation.[15] Two situations have been considered with the same concentration in volume (1%) and the same relative refractive index ($m=0.858$): (i) Rayleigh, with $ka=0.232$, $\sigma_t=2.19\times10^{-6}$ μm^2, $\ell=19.1$ mm, $\langle\cos\theta\rangle=0.008\,24$, and $k\ell=444\,084$, and (ii) large spheres, with $ka=23.2$, $\sigma_t=4.88$ μm^2, $\ell=0.0859$ mm, $\langle\cos\theta\rangle=0.931$, and $k\ell=1900$.

1. Reflection

In reflection we have compared the numerical simulation result with the experimental one in Fig. 2. We have also considered a slab with thickness $L/\ell^*=15$ and three regimes of scattering, pointlike scatterers (Ray-

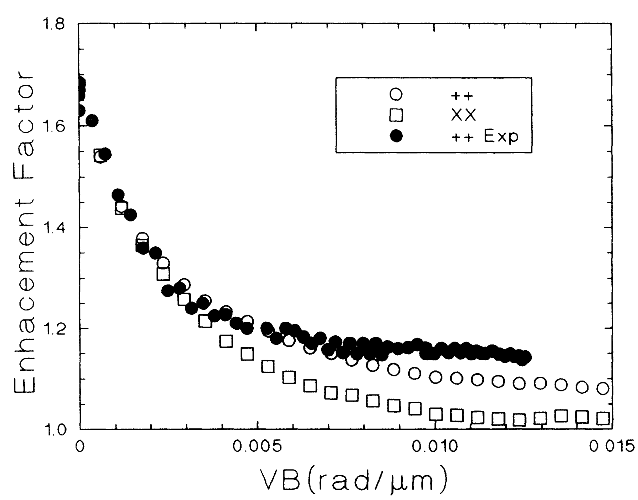

FIG. 2. Comparison between the calculated (numerical simulation) enhancement factor in the $++$ polarization channel and xx channel and the $++$ channel experiment [the experimental points have been obtained by Lenke and Maret (Ref. 23)]. The parameters are: $\lambda_{\text{vac}}=0.4579$ μm, $a=0.1$ μm, leading to $ka=2.32$ and $n_s=1.45$, $n_m=1.65$, leading to $n_s/n_m=0.858$. In the experiment the value of L/ℓ^* is about 500 and in the simulation the value is of $L/\ell^*=15$. As discussed in Ref. 14, the value of the Verdet constant depends on the magnetic field in the experiment with the starting value of $V=1571$ rad/mT. In the simulation we have considered $V=157.1$ rad/mT. To fit the experimental data we have used the scale $(VB)_{\text{exp}}=3.5(VB)_{\text{sim}}$ and $(EF)_{\text{exp}}=(EF)_{\text{sim}}$.

leigh regime with $ka=0.232$), intermediate regime ($ka=2.32$), and large spheres ($ka=23.2$). In all regimes we have considered incident light polarized circularly and linearly along the x direction. For both cases, we have obtained the enhancement factor for the same polarization channel ($++$ or xx) and for the opposite one ($+-$ or xy). We have observed that the enhancement factor presents some general properties (Fig. 3).

(1) The enhancement factor in the $+-$ channel is independent of B in all cases. As we have seen in Sec. I D, this invariance of the opposite-helicity channel has been predicted analytically by MacKintosh and John[7] and here verified numerically.

(2) For small values of VB and for the same polarization channel, either $++$ or xx, the enhancement factor decays exponentially with the same attenuation constant. This attenuation depends on the size of the scatterers. This behavior has also been observed experimentally by Lenke and Maret.[23]

(3) For large values of VB, the enhancement factor does not converge to 1: their asymptotic values are different and depend on the size of the spheres. This convergence to nontrivial asymptotic values has also been observed experimentally.[23] These asymptotic values as a function of the size parameter ka are represented in Table II.

Let us start the discussion for the small values of VB. The exponential decays observed in Figs. 3(a), 3(b), and (3c) can be understood qualitatively in the framework of the Rayleigh model (Sec. III B). For large values of VB, we see from Table II that the asymptotic values of the enhancement factor in the xx, xy, and $++$ polarization channels increase as the size parameter ka increases. On the other hand, the value of the enhancement factor of the $+-$ channel tends to decrease as the parameter ka increases. We see that these values of the enhancement factor cannot be explained by the proportion of single, double, or triple scatterings. To understand qualitatively these results we have to take into account the multiple scattering of light through the path-length distribution.

The path-length distribution in reflection is roughly described by a power-law [$P(s)\propto s^{-3/2}$] which does not have any characteristic length. It allows very long sequences which are not very numerous. These long sequences dephase the direct and reverse sequences through the azimuthal randomization (ϕ randomization) and backward scatterings. The ϕ randomization affects drastically the linear polarization states while the backward scattering changes the helicity of the wave, so that these long sequences tend to push the enhancement factor down to 1. On the other hand, this distribution allows very many short paths, typically of the length of $\ell^*=\ell/(1-\langle\cos\theta\rangle)$. If the scatterings are strongly peaked forward, the backward scattering is a very rare event. These short sequences do not have enough scatterings to dephase significantly the direct and reverse sequences, and they tend to preserve the helicity of the waves.

Let us now consider very anisotropic scatterings where $ka=23.2$ [Fig. 3(c)]. The scattering amplitudes are strongly peaked forward. Because of the azimuthal ran-

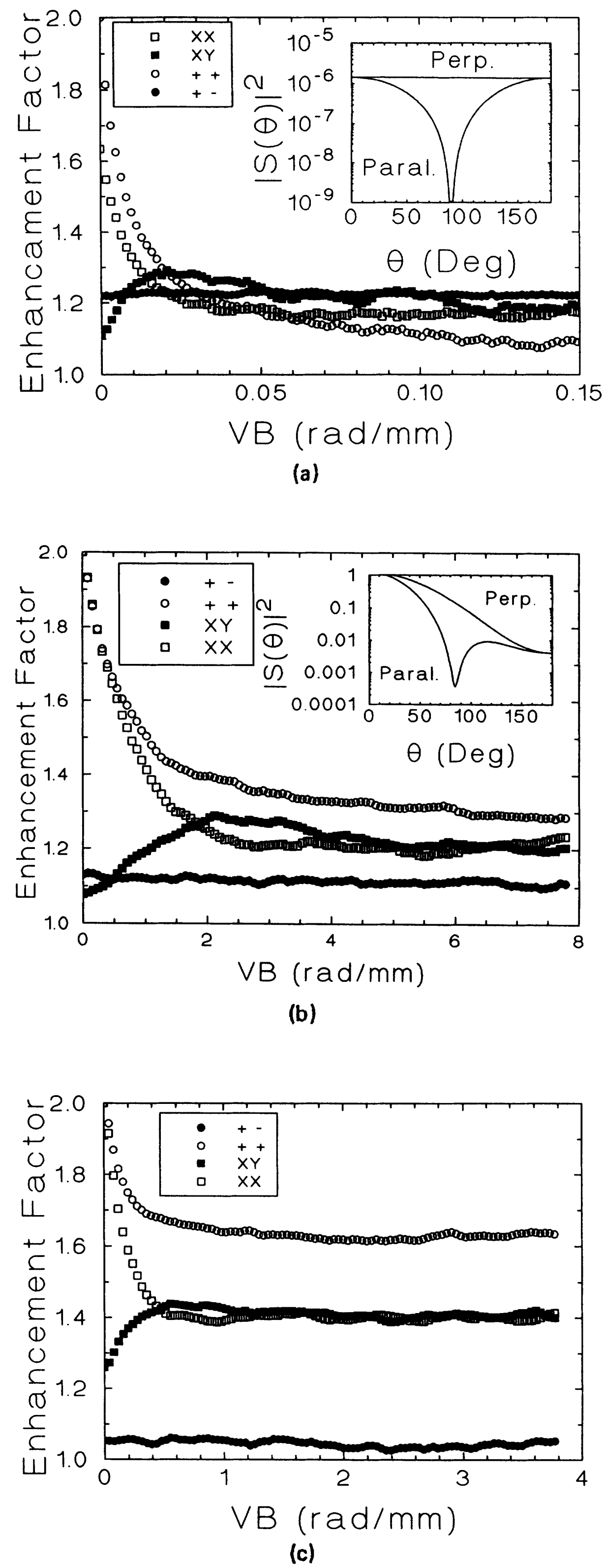

FIG. 3. The enhancement factor obtained by the Monte Carlo simulation in the $++$, $+-$, xx, and xy polarization channels as a function of VB for a slab of thickness $L/\ell^*=15$. The considered regimes are (a) Rayleigh ($ka=0.232$), (b) Mie ($ka=2.32$), and (c) large spheres ($ka=23.2$). The refractive index ratio is $n_s/n_m=0.858$. Insets: the parallel and perpendicular scattering amplitudes as a function of the scattering angle.

TABLE II. Asymptotic values of the enhanced factor for strong magnetic fields.

ka	$\langle\cos\theta\rangle$	Single scattering	Double scattering	Triple scattering	xx	xy	$++$	$+-$
0.232	0.008	18.4%	10.3%	7.36%	$\cong 1.15$	$\cong 1.15$	$\cong 1.05$	$\cong 1.20$
2.32	0.689	1.31%	2.48%	3.22%	$\cong 1.25$	$\cong 1.25$	$\cong 1.35$	$\cong 1.10$
23.2	0.931	0.107%	0.123%	0.134%	$\cong 1.40$	$\cong 1.40$	$\cong 1.60$	$\cong 1.05$

domization, any incident linear polarization state will be scattered into other linear polarization states. So the x direction has roughly the same probability to be visited as the y direction after ℓ^*/ℓ scatterings. This is the reason why the enhancement factors of the xx and xy channel have the same asymptotic values. On the other hand, the backward scatterings are very rare, and the helicity is preserved. This is why the enhancement factor of the $++$ channel is larger than that of the $+-$, which is very close to 1.

For $ka=2.32$ [Fig. 3(b)], the scatterings are still anisotropic, but the scattering amplitudes are not so forward peaked as in the previous case. Backward scatterings occur more often so that they tend to increase the enhancement factor of the $+-$ channel and to decrease the factor of the $++$ channel, which is still larger than the $+-$ one.

For the Rayleigh scattering $ka=0.232$ [Fig. 3(a)], the forward and backward scatterings have the same probability to occur. A helicity flip is not a rare event, pushing the asymptotic value of the enhancement factor of the $++$ channel to a value smaller than the channel $+-$. We notice that because of the single scattering the enhancement factor of the xx channel is smaller than 2.

2. *Transmission*

For transmission, the intensity correlation functions for incident circular and linear polarization along the x direction are shown in Fig. 4. In the diffusion limit (Fig. 4) $L/\ell^*=7$, 8, 9, 10, and 11, VBL is a good reduced variable, according to the random-helicity model and Rayleigh theory [Eqs. (3.1a) and (3.16c)] for small values of VBL. For larger values of VBL, $G_{xx}^{(2)}(B)$ cannot be written only in terms of VBL. This is apparent from Fig. 4 where oscillations are observable above the noise. For thick slabs and for small values of VBL, no information about the characteristic lengths due to the Faraday effect can be obtained.

For the intermediate regime, we have plotted $G_{xx}^{(2)}$ as a function of VB for $L/\ell^*=2$, 3, 4, 5, and 10 for linear and circular incidence. For small values of L/ℓ^* the correlation function displays net oscillations [Figs. 5(a)

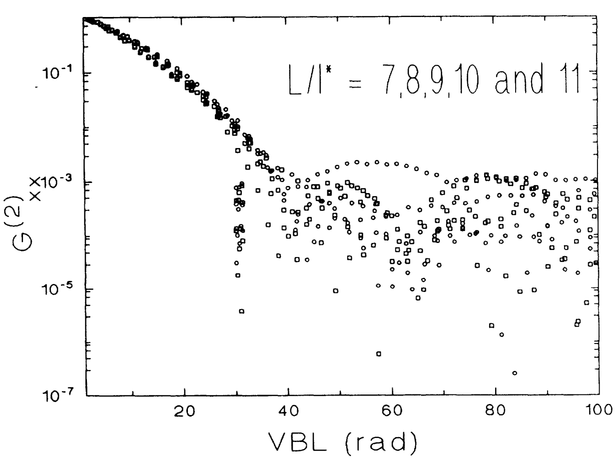

FIG. 4. Intensity correlation for the Mie scatterers for incident linear and circular polarized light as a function of VBL. The refractive index ratio is $n_s/n_m=0.858$ and the size parameter is $ka=2.32$. The slab thicknesses considered are $L/\ell^*=7$, 8, 9, 10, and 11.

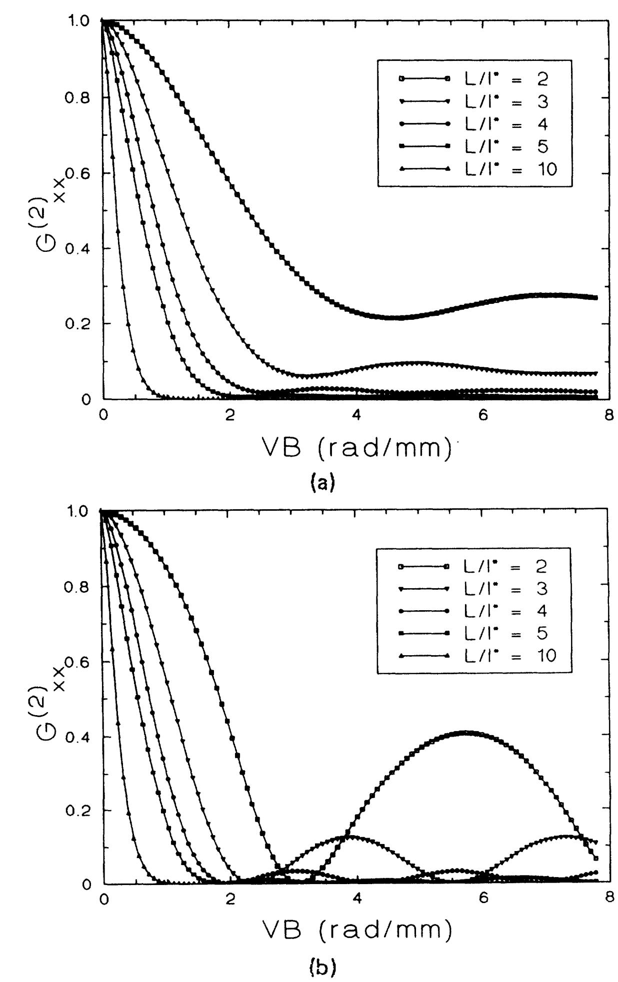

FIG. 5. Intensity correlation as function of VB for incident (a) circular and (b) linear polarized light for slabs of thickness $L/\ell^*=2$, 3, 4, 5, and 10. The other parameters are the same as in Fig. 4. The lines are only a guide to the eyes.

and 5(b)] which do not exist in a homogeneous slab (no scatterings) where $G_{xx}^{(2)}=1$. Another feature is that the amplitudes of these oscillations are not damped for larger VB [see curves for $L/\ell^*=3$ and 4 in Fig. 5(b)].

Contrary to the oscillations calculated in the Rayleigh regime which are exponentially damped [Eq. (3.16d)], the oscillations observed in the Mie regime have the same amplitude and the same period as the magnetic field is increased. These oscillations are essentially due to the coherent beam and to single scattering. Another mechanism to explain these oscillations is the one-dimensional behavior. For thinner slabs, because of anisotropy, the scattering paths are almost straight lines. This is relevant to the Faraday effect in a chain, where the photon executes a one-dimensional random walk. In this model, the polarization states rotate in the same sense between the successive scatterings, which can be either forward or backward, leading to an accumulation of the rotation angle proportional to the total length of the path. This mechanism is also observed for incident circular polarization. We recall that the paths are not strictly speaking straight lines, so that the incident circular state becomes an elliptical one; this ellipticity is amplified by the multiple scattering. The effect of the magnetic field is to turn these ellipses and the correlation function decays. For large VB it presents oscillations.

DISCUSSION AND CONCLUSION

Several important properties of the multiple scattering of waves can be understood in the simplified frame of the scalar theory. The intensity enhancement of the backscattering cone is due to the existence of reverse sequences which interfere with the direct ones. Hence, for scalar waves, where only the phase difference between the direct and reverse sequence is taken into account, it is correct to claim that these sequences are coupled by a time-reversal operation. This basic interference, due to the reciprocity principle, is very robust: neither absorption nor confinement in finite slabs can affect the value 2 of the enhancement factor (if single scattering is excluded). The role of absorption or finite slabs is to round off the peak of the cone by cutting off the long scattering sequences (which give rise to the sharp peak of the cone).

When the vectorial nature of light is taken into account, the situation is more complex. If the multiply scattered light is detected in the same polarization channel as the incident light (xx or $++$ configurations), the direct and reverse sequences interfere constructively giving the factor 2 of the cone. On the other hand, for the opposite polarization channel (xy or $+-$), the enhancement factor is smaller than 2, since the final polarization states are different, breaking the reciprocity between the direct and reverse sequences. These properties are expressed mathematically by a simple transposition operation of the effective Jones matrix (which describes the multiple-scattering process) written in the circular basis or an antitransposition for the Jones matrix written in the linear basis.

The Faraday effect is known to break the time-reversal symmetry and reciprocity principle for a single scattering. For a sequence, it introduces the rotation of polarization between successive scatterings. Between two scatterings, the Faraday angle has opposite sign between the direct and reverse sequences, but these rotations happen in different local frames which are conjugated by an improper rotation operation. The time-reversal symmetry is always broken by the Faraday effect, but it is the reciprocity-principle breaking between the direct and reverse sequences that alters the enhancement factor of the scattering cone. To exemplify this statement, consider an optically two-dimensional medium and circular scatterers. The Jones matrix of each single scattering is diagonal and the product of these matrices is diagonal. The enhancement of the same polarization channel always exists but the intensity in the opposite channel is always null since these components are not connected by the diagonal matrix. The presence of a magnetic field introduces the rotation matrices between successive scatterings: then the effective Jones matrix is no longer diagonal and a close analogy with the problem in three dimensions without magnetic field can be made by replacing α by $-\phi$. As in the three-dimensional problem with $B=0$, the backscattering cone in two dimensions, for the same polarization channel, is not altered by the magnetic field, but the opposite polarization channel is affected.

Although the random-helicity model offers a simple frame for the analysis of the main properties of the multiple scattering of light, some important features are not well founded in this model and call for a detailed analysis. This deeper analysis is the principal motivation of this work. The first objection against this model is certainly the fact that the randomness of the polarization state is not justified as an independent random variable of the wave vector. Actually, the wave vectors are the basic and unique random variables of the multiple-scattering problem. This remark is crucial in the one-dimensional problem. In this model, a complete correlation occurs between the polarization rotation and the length of the diffusion paths, while the wave vectors are totally randomized by the one-dimensional random walk. An analytical calculation of this situation shows that the correlations are damped only by the dispersion of the path-length distribution rather than by any randomness of the polarization states. The second objection to the random-helicity model is that the problem of the successive rotations of the polarization vectors by the Faraday effect *must* be handled by a matrix formalism. The nth-order multiple scattering is mapped mathematically into a matrix power problem. It solution involves the research of the largest eigenvalue. The damping of the correlation function originates from the transition between the polarization states coupled to the scattering wave vector rather than independent random transitions of the polarization. Indeed, there is no scalar analogy of the problem of the vector rotation in three dimensions.

By a recurrence method, we have succeeded in obtaining the characteristic attenuation factor in the scattering-number representation for Rayleigh scatterers. We have found both exponential dampings which are experimentally observed and oscillatory correlations as a function of the magnetic field. These oscillations should be observed in the intermediate regime, between the single-scattering and the diffusion regime. By our numerical simulations for Mie scatterers, the main results are confirmed qualitatively; exponential (Gaussian) damping of the correlation function in transmission for the diffusive regime as well as oscillatory behavior for larger magnetic fields and a moderate number of scatterings. For reflection, the damping of the backscattering-cone enhancement factor is well accounted and compared with the experiments. For stronger magnetic fields nontrivial values are observed for this factor. These values correspond to the contribution of the short paths or low order of scatterings, proving that the correlation between the direct and reversed sequences is maintained even in high magnetic fields. Finally, experiments for two-dimensional systems could discriminate between the simple analysis of the random-helicity model and the present analysis. Furthermore, the oscillatory behavior of the intensity correlation function for thinner slabs, far away from the diffusion regime, is a feature of the Faraday effect in the context of the multiple scattering of light that has not been examined experimentally.

ACKNOWLEDGMENTS

We thank F. Erbacher, R. Lenke, G. Maret, J. M. Luc, T. M. Nieuwenhuizen, and B. van Tiggelen for very stimulating discussions. One of us (A.S.M) also wishes to thank CAPES-Brazil for financial support.

---

*Present address: Université de Genève, Groupe de Physique Appliquée, 20, r. de l' école de Médicine, CH-1211 Genève 04, Switzerland.

[1] *Classical Wave Localization,* edited by P. Sheng (World Scientific, Singapore, 1990).

[2] *Mesoscopic Phenomena in Solids,* edited by B. L. Altshuler, P. A. Lee, and R. A. Webb (North-Holland, Amsterdam, 1991).

[3] E. Akkermans, P. E. Wolf, and R. Maynard, Phys. Rev. Lett. **56**, 1471 (1986).

[4] H. C. van de Hulst, *Light Scattering by Small Particles* (Dover, New York, 1981).

[5] A. S. Martinez and R. Maynard, in *Photonic Band Gaps and Localization,* edited by C. M. Soukoulis (Plenum, New York, 1993), p. 99.

[6] A. A. Golubenstev, Zh. Eksp. Teor. Fiz. **86**, 47 (1984) [Sov. Phys. JETP **59**, 26 (1984)].

[7] F. C. MacKintosh and S. John, Phys. Rev. B **37**, 1884 (1988).

[8] F. A. Erbacher, R. Lenke, and G. Maret, Europhys. Lett. **21**, 551 (1993).

[9] A. S. Martinez and R. Maynard, in *Soft Order in Physical Systems,* edited by R. Bruinsma and Y. Rabin (Plenum, New York, in press).

[10] P. S. Theocaris and E. E. Gdoutos, *Matrix Theory of Photoelasticity* (Springer-Verlag, New York, 1979).

[11] S. Chandrasekhar, *Radiative Transfer* (Clarendon, Oxford, 1950); Z. Sekera, J. Opt. Soc. Am. **56**, 1732 (1966).

[12] R. L.-T. Cheung and A. Ishimaru, Appl. Opt. **21**, 3792 (1982).

[13] C. Prada, F. Wu, and M. Fink, J. Acoust. Soc. Am. **90**, 1119 (1991).

[14] F. A. Erbacher, R. Lenke, and G. Maret, in *Photonic Band Gaps and Localization* (Ref. 5), p. 81.

[15] R. Lenke and G. Maret, Physica Scripta **T49**, 605 (1993).

[16] A. S. Martinez and R. Maynard (unpublished)

[17] E. Akkermans, P. E. Wolf, R. Maynard, and G. Maret, J. Phys. (Paris) **49**, 77 (1988).

[18] G. Grehan and G. Gouesbet, Appl. Opt. **18**, 3489 (1979).

[19] W. J. Lentz, Appl. Opt. **15**, 668 (1976).

[20] E. A. Bucher, Appl. Opt. **12**, 2391 (1973).

[21] K. E. Kunkel and J. A. Weinman, J. Atmos. Sci. **33**, 1772 (1976).

[22] P. Bruscaglioni and G. Zaccanti, in *Scattering in Volumes and Surfaces,* edited by M. Nieto-Vesperinas and J. C. Dainty (Elsevier, Amsterdam, 1990).

[23] R. Lenke and G. Maret (private communication).